# EVALUATING POST-EARTHQUAKE FUNCTIONALITY AND SURGE CAPACITY OF HOSPITAL EMERGENCY DEPARTMENTS USING DISCRETE EVENT SIMULATION

by

Gerald M. Palomino Romani

B.Sc., National University of Engineering (Peru), 2016

A THESIS SUBMITTED IN PARTIAL FULFILLMENT OF

THE REQUIREMENTS FOR THE DEGREE OF

MASTER OF APPLIED SCIENCE

in

THE FACULTY OF GRADUATE AND POSTDOCTORAL STUDIES

(Civil Engineering)

THE UNIVERSITY OF BRITISH COLUMBIA

(Vancouver)

November 2021

The following individuals certify that they have read, and recommend to the Faculty of Graduate and Postdoctoral Studies for acceptance, the dissertation entitled:

Evaluating post-earthquake functionality and surge capacity of hospital emergency departments using discrete event simulation.

submitted by Gerald M. Palomino Romani in partial fulfillment of the requirements for

the degree of Master of Applied Science

in Civil Engineering

**Examining Committee:**

Carlos Molina Hutt, Department of Civil Engineering, The University of British Columbia
Supervisor

Luis Ceferino, Department of Civil and Urban Engineering, New York University
Supervisory Committee Member

## Abstract

Past earthquakes have illustrated the impacts of reduced hospital functionality due to physical damage resulting in a health service deficit immediately after a major seismic event. In this paper, a methodology was developed to quantify the deficit in health care anticipated due to a loss of functionality of a hospital emergency department (ED) and a surge in demand due to regional damage in an earthquake scenario. Earthquake-induced patient arrivals were calculated using multi-severity casualty estimation for the catchment area of the hospital. The surge in patients was then compared to the ability of the hospital to treat patients (capacity) based on anticipated functionality. Nonlinear response history analysis of the hospital building was performed using simplified structural models, and the structural and nonstructural component damage was estimated based on FEMA P-58. Expected damage was linked to the post-earthquake functionality of the ED services areas on each floor by incorporating the fault tree analysis method. Lastly, Discrete event simulation was utilized to evaluate the ED surge capacity, providing hospital performance metrics such as wait times (WT) and length of stay (LOS) for patients of ranging acuity. A case study of a hospital in the City of Vancouver subjected to an Mw9.0 Cascadia Subduction Zone scenario earthquake was presented. Emergency rooms were identified as the ED bottleneck during the emergency response. The mean ER WT exceeded its limit of two hours and reached up to 17 hours in the most unfavorable simulation. Likewise, the mean LOS nearly doubled from 6.5 to 12 hours, also exceeding the established target of 10 hours. The deployment of field hospitals for less severe patients as an emergency plan to mitigate the ED overcrowding was also analyzed to demonstrate that the methodology can be used as a decision support tool to improve healthcare disaster planning.

## Lay Summary

Healthcare infrastructure plays a key role in the recovery of communities in a post-disaster scenario. In this thesis, a methodology is proposed to simulate the patient flow through a hospital emergency department (ED) in a post-earthquake scenario. The results from the simulations allow estimating valuable information such as the post-earthquake functionality, patient surge, and operability of the ED in terms of commonly used hospital performance metrics (e.g., patient wait time and length of stay). To illustrate the methodology, a case study hospital in the City of Vancouver subjected to a plausible $M_w$9.0 Cascadia Subduction Zone earthquake scenario is presented. The ED post-earthquake functionality and the surge capacity during the emergency response are evaluated. The model developed was also utilized to investigate the effect of possible improvements within the ED. This proposed methodology can support decision-making in support of more effective emergency response plans and enhanced seismic hospital resilience.

## Preface

The author of this thesis was responsible for reviewing the literature, developing the methodology, computer programming, data processing, conducting analyses, and interpreting the results with support from his advisor, Prof. Molina Hutt. The thesis was drafted by the author and finalized in an iterative review process with Prof. Molina Hutt. The author of this thesis was responsible for preparing the tables and figures.

A version of Chapters 1, 3, and 4 have been submitted for publication as a journal manuscript: Palomino Romani G., Blowes K., and Molina Hutt C. (n.d.) “Evaluating post-earthquake functionality and surge capacity of hospital emergency departments using discrete event simulation”, which is currently under peer review. K. Blowes contributed to the formulation of the methodology presented in Chapter 3; and improved the presentation of the results, including figures, tables, and writing edits. C. Molina Hutt assisted in the concept formation, manuscript composition, writing and supervised the work throughout the research. I did the literature review, developed the codes to perform the analyses, prepared the first draft of the manuscript, and interpreted the results.

# Table of Contents

## List of Tables

## List of Figures

## Acknowledgments

I would like to express my most sincere gratitude to my supervisor, Prof. Carlos Molina Hutt, who provided me with the opportunity to be part of his great research team. I would like to thank him for his excellent guidance and continued support, always offered in a positive constructive manner during every step of my research at the University of British Columbia (UBC). I am truly honored to have worked under his supervision. Special thanks are owed to Prof. Luis Ceferino from New York University for his selfless support since I held onto my goal to study for a master's. His guidance allowed me to work on topics in which I have always had tremendous interest.

I offer my enduring gratitude to the faculty, staff, and my fellow students at UBC, who have inspired me to continue my work in this field. I owe particular thanks to my research colleague and friend Kristen Blowes for her insightful input throughout this research work. I would also like to thank Abbie Wen, Preetish Kakoty, Pouria Kourehpaz, and Camilo Granda for their help and support over the course of my graduate studies.

This research was funded by MITACS Accelerate in partnership with Vancouver Coastal Health and Bush Bohlman & Partners LLP under project No. IT16440. I am specifically highly grateful to Tim White (Bush Bohlman & Partners LLP), Alan Lin, and the Decision Support team (Vancouver Coastal Health) for providing relevant data essential to perform this research. I would also like to thank the M9 team at the University of Washington for sharing the results of their M9 simulations in southwest British Columbia, and Natural Resources Canada for sharing the necessary exposure data used to perform the regional risk assessment. Finally, I would also like to acknowledge Dr. Harry King, developer of the free open-source simulation software JaamSim, for addressing my queries.

## Dedication

*This thesis is dedicated to my parents and my sister who have supported me throughout my years of education.*

# Chapter 1: Introduction

## 1.1 Motivation and background

Following a natural disaster, a key step in emergency response is ensuring the medical treatment of the affected population. Since emergency departments (ED) are the first points of admission of injured people, the effective functioning of EDs is critical in the effort to save lives after a large earthquake (Gul and Guneri, 2015b). When a disaster occurs, the number of patients who require treatment in EDs may increase by up to five times the steady-state volume in a short time frame (Henderson *et al.*, 1994), often exceeding the surge capacity of a well-functioning hospital ED. Further, damage to the hospital building may lead to the partial or total loss of functionality of the ED, thereby reducing the ability of healthcare professionals to treat patients. As illustrated in Figure 1.1, both factors (the increase of the demand and the reduction in hospital capacity) can generate a health service deficit that will hinder the timely and efficient treatment of patients (Ceferino, 2019).

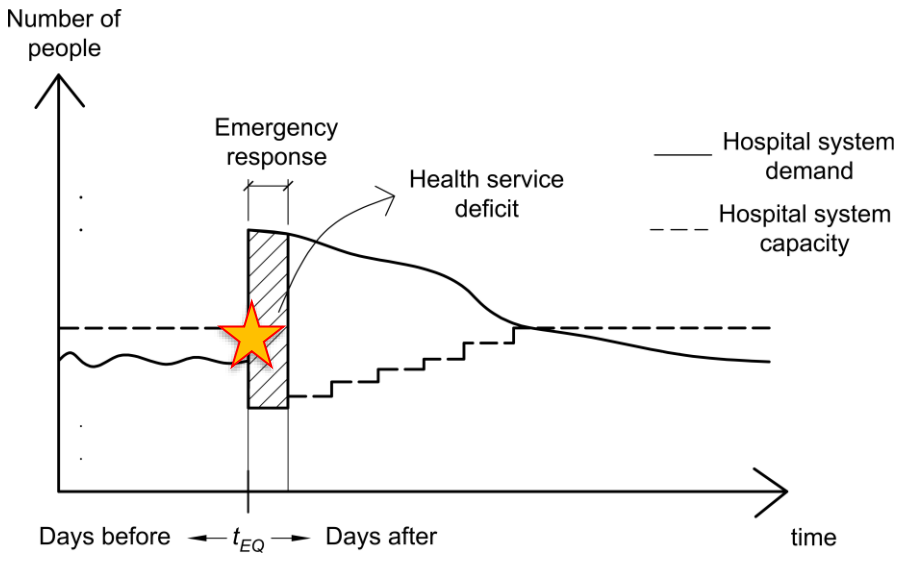


**Figure 1.1 Demand and capacity of health care before and after an earthquake (Ceferino, 2019).**

The complexity and uncertainty of ED operations and workflow raise additional challenges such as prolonged wait times, inefficient use of ED resources, and unbalanced staff scheduling (Paul and Lin, 2012). To evaluate ED operations and quality of service, performance metrics such as wait time, length of stay, and resource utilization can be used. Wait time is considered a critical metric since it is directly related to the quality of service (Cimellaro, Reinhorn, and Bruneau, 2010). To measure these indicators, simulation modeling methods to account for the dynamic behavior of health care systems have been developed (Cimellaro *et al.*, 2008; Ouyang, 2014). These computer simulations are an appropriate method to investigate ED operations during disaster events and they can be used effectively as a decision support tool (Gul and Guneri, 2015a).

System dynamics (SD), agent-based simulation (ABS), and discrete event simulation (DES) are modeling techniques commonly used to analyze ED operations. Gunal (2012) presented a technical comparison of the three methods from a hospital modeling perspective. Continuous simulation modeling, a form of SD, is useful for providing a framework for evaluating the link between EDs to look at strategic-level problems, and thus is more appropriate for studying hospital network systems instead of individual EDs. ABS is an emerging method that focuses on the interactions between autonomous agents (patients and healthcare workers) and has been mainly used to build agent-based decision support systems such as models to optimize the ED staff configuration. These methods are not well suited for modeling the complexity and stochastic nature of an ED, where the interest is in several distinct events and their durations. DES is a well-established method in this domain due to its ability to model discrete, stochastic, and process-oriented systems with a visual representation of individual patient flows and queue forming (Paul,

Reddy, and Deflitch, 2010). DES modeling is included in the proposed methodology to evaluate the seismic performance of health care facilities, namely EDs.

While extensive research on ED simulation has been performed, Gul and Guneri (2015a) noted that much of the current literature focuses on the need to improve the efficiency of the ED resources and processes under normal conditions. Despite this, several key studies have investigated the performance of EDs during disaster events (Yi *et al.*, 2010; Gul and Guneri, 2015a; Ceferino *et al.*, 2020; Yu, Zhai, and Wen, 2020; and Lin, Lin, and Lin, 2021). However, limited studies account for the anticipated ED functionality loss due to facility damage after a disaster. For instance, Cimellaro, Reinhorn, and Bruneau (2010) developed an ED simulation model using DES that incorporates the influence of physical damage by penalty factors that are applied to all internal parameters of the hospital (e.g., emergency rooms, operating rooms, and bed capacity). Favier *et al.* (2019) used DES and accounted for ED functionality loss by incorporating a probabilistic framework developed by Kuo *et al.* (2008) for the emergency rooms and a deterministic approach using binary states developed by Vásquez *et al.* (2017) for the operating rooms. While these studies have proposed approaches to account for the ED capacity reduction, one of the major limitations is that the ED post-earthquake functionality is assumed to be controlled by a limited number of components; also, only a limited number of ED services areas were assumed to lose functionality. Notably, Yavari *et al.* (2010) introduced a methodology for anticipating the post-earthquake functionality of hospitals that accounts for the interdependencies of hospital systems (structural, non-structural, lifelines, and personnel). Similarly, Jacques *et al.*, (2014) proposed the use of fault-tree analysis to relate the physical damage, loss of supplies, and staff availability to the post-earthquake functionality loss of critical healthcare services. Thus, a current research gap in the simulation of EDs during an earthquake disaster is the implementation of a detailed functionality

loss assessment, as the above-mentioned, that enables the evaluation of the micro-level behavior of EDs using performance metrics.

The goal of this study is to assess the seismic resilience of hospitals by developing a generic DES model that accounts for the ED functionality loss by incorporating the framework developed by Yavari *et al*. (2010) to evaluate the ED surge capacity in terms of commonly used hospital performance metrics. The novelty of the proposed methodology lies in: (1) accounting for the damage to a wide range of structural and non-structural components and the interdependencies between hospital systems in the functionality loss calculation; (2) incorporating simplified nonlinear structural analysis models capable of providing rapid estimates of the engineering demand parameters (EDPs) in each floor of the hospital buildings; making the method suitable to analyze multiple EDs in a regional scale; (3) capturing the inherent variability of the demand surge and capacity estimation by employing ground motion intensity maps, and consistent acceleration time histories in a scenario-based framework; and (4) enabling the evaluation of the ED performance through metrics such as wait times on relevant service areas, and the length of stay according to patients acuity.

## 1.2 Objectives

This thesis aims to develop a framework to evaluate the post-earthquake functionality and surge capacity of emergency departments (EDs) using discrete event simulation (DES). The focus of this study is the emergency response phase, which can span from the first hours to a few days after the earthquake. During this period, recovery of the hospital ED functionality is not likely to be completed. The methodology developed aims to support decision-makers to improve the reliability of existing emergency response plans. The main objectives of this research are:

A. To develop a methodology able to quantify the health care deficit (expressed in terms of demand-to-capacity ratio as a function of patient wait times) anticipated due to a loss of functionality of a hospital ED and a surge in demand due to regional damage and the associated injuries in an earthquake scenario.
B. To explicitly account for the functionality loss of the ED services areas on each floor due to the structural and non-structural damage of a hospital building after an earthquake.
C. To incorporate the discrete event simulation technique into the seismic risk assessment framework to model the flow of patients through an ED during an earthquake scenario.
D. To enable the evaluation of the ED performance metrics, such as wait times and length of stay of patients, and to provide estimates of the overall ED surge capacity after an earthquake scenario.

A case study was conducted to demonstrate the applicability of the proposed framework. It was demonstrated that the methodology can be utilized as a decision support tool to improve healthcare disaster planning. Further, while the model developed focused on a specific ED, it can be replicated and applied to any other ED.

### 1.3 Organization

This thesis is organized into five chapters and two appendices, as described in the following paragraphs.

Chapter 1 includes the motivation of this work, provides an introduction, and presents the objectives to be addressed.

Chapter 2 provides a literature review on (i) seismic resilience of health care facilities, including an introduction of the simulation modeling techniques available, and (ii) computational modeling for seismic damage simulation, with a focus on simplified numerical models.

Chapter 3 presents the proposed methodology and provides the details of each step required to determine the demand and capacity of health care after an earthquake. The method integrates both factors into a DES simulation model to quantify the post-earthquake surge capacity of an ED. The risk outputs are expressed in terms of commonly used hospital performance metrics.

Chapter 4 presents a case study hospital in the City of Vancouver subjected to 30 $M_w$9.0 Cascadia Subduction Zone (CSZ) earthquake scenarios to demonstrate the applicability of the methodology. A simple mitigation measure is also used to demonstrate the benefits of the proposed methodology to quantify the impact of different interventions. A discussion of the results is provided in this chapter.

Chapter 5 summarizes the key findings, as well as the limitations of this work. It also provides recommendations for future research.

Appendix A provides a detailed explanation of the procedure to build a nonlinear simplified model of a 12-story RC shear wall building and its validation against a refined finite element model. Finally, Appendix B presents further details of discrete event simulation modeling, with a focus on the case study ED presented in Chapter 4, to illustrate the procedures followed.

# Chapter 2: Literature Review

## 2.1 Modeling capacity of healthcare facilities

Health care facilities have been recognized as strategic buildings in hazardous events and play a key role in disaster response and recovery. When a disaster occurs, injured people immediately go to the nearest hospital emergency department (ED) for medical assistance; thus, it is critical that hospitals maintain their function. A hospital's ability to supply essential health services and continued functionality when an emergency or disaster occurs, is referred to as surge capacity (Watson *et al.*, 2013). Developing surge capacity is a matter of managing healthcare supply and demand, and it is dependent on the efficiency of the emergency response plan implementation. Adams (2009) identified the key components of surge capacity, referred to as the four S's: staff (i.e., clinical personnel), stuff (i.e., supplies and equipment), structure (i.e., physical space), and systems (i.e., policies and procedures). These same factors are taken into account when evaluating the functionality of critical hospital services.

After a large earthquake, emergency response plans must be activated to maintain functionality, or if possible, temporally increase the capacity (e.g., deployment of field hospitals) to meet the needs of patients with life-threatening injuries in a timely manner. At short notice, hospital EDs must provide care to an increased number of patients due to earthquake-related injuries (e.g., falling damaged components, building collapse). However, this increase in patient volume, in conjunction with the decreasing ED functionality due to the anticipated damage, usually exceeds the surge capacity of any well-functioning hospital. As such, methods are needed to evaluate the post-earthquake functionality and surge capacity of EDs and to express this

performance in a meaningful way in order to inform emergency preparedness and response planning.

### 2.1.1 Hospital resilience

Hospital resilience is a comprehensive concept that can be defined as "hospital's capability to resist, absorb, respond to the shock of disasters while still retaining their most essential functionality (e.g., prehospital care, emergency medical treatment, critical care, decontamination, and isolation), then recover to its original state or a new adaptive state" (Zhong *et al.*, 2014). To evaluate disaster resilience, the Multidisciplinary Center for Earthquake Engineering Research (MCEER) introduced four criteria: robustness, resourcefulness, redundancy, and rapidity (Bruneau *et al.*, 2003). Zhong *et al.* (2013) adopted these criteria and integrated them into the four domains of hospital resilience: (1) safety and vulnerability, (2) preparedness and resources, (3) continuity of essential services, and (4) recovery and adaptation. In this context, the present thesis aims to develop a method to address the safety and continuity aspects of hospital EDs by evaluating the functionality and surge capacity following a major earthquake.

Researchers have developed different metrics to quantify resilience at a community scale (Bruneau *et al.*, 2004; Miles and Chang, 2006; O'Rourke, 2007; Reed *et al.*, 2009). For hospitals, resilience can be measured in terms of the level of hospital function over time. The hospital function has been defined in many different ways. For instance, Cimellaro *et al.* (2008) developed a framework to quantify disaster resilience of hospital systems employing functionality loss estimation and recovery models. The hospital's resilience was expressed in terms of quality of service, which was directly derived from patients' wait times. Meanwhile, Jacques *et al.*, (2014) proposed a resilience metric that is calculated as a function of the number of services offered, a redistribution function, and the loss of functionality obtained from fault-tree analyses. A different

approach consists of relating the seismic resilience to the number of patients per day that can be treated as a measure of the capacity of healthcare facilities (Bruneau and Reinhorn, 2007). This method is adopted in the present thesis, as the estimation of 'patient per day' capacity can be directly related to the functionality of the physical space within an ED. This approach is suitable for engineering quantification because it focuses on the probable damage to physical infrastructure (structural and nonstructural components) and its ability to provide the intended function.

### 2.1.2 Other definitions

Because of the importance of maintaining healthcare capacities during normal and disaster conditions, different methodologies have been developed to evaluate the post-earthquake functionality and surge capacity of EDs. To better understand the methodology presented in Chapter 3, it is important to acknowledge the following terms and definitions commonly used in the literature and also adopted in this study:

- Emergency Management: It is the administration of resources and responsibilities to deal with hazards, risks, and disasters of all types and scales. It includes pre-event (preparedness and mitigation) and post-event (response and recovery) activities (FEMA, n.d.).
- Demand: ED demand is defined as the number of patients that visit an ED to receive medical treatment. The demand varies during the day and is typically expressed in terms of patient arrival rates (pat./hour). A sudden increase in demand is referred to as a surge.
- Capacity: ED capacity is defined as the number of injured patients that can be effectively treated without causing unacceptable (i.e., life-threatening) patient waiting times (Yi *et al.*, 2010). In this study, hospital capacity is expressed in terms of the critical arrival rate, a threshold above which effective treatment can no longer be provided.

- Surge Capacity: The ability of a hospital ED to accommodate patients considering its increased or decreased capacity when mass casualties occur as a consequence of disasters such as earthquakes. In this work, surge capacity is evaluated in terms of performance metrics, including the hospital demand to capacity ratio, during the emergency response phase, which may span from a few hours to a few days after the earthquake event.
- Overcrowding: It is the situation in which the healthcare demand exceeds the ED capacity. Consequently, it diminishes the ED's ability to provide quality services within a reasonable time. Moreover, evidence suggests that it reduces the efficiency of ED operations, and hence prolongs the length of stay of all patients (Morley *et al.*, 2018). Overcrowding is caused by multiple factors, including a surge of patients, laboratory delays, shortage of resources, and management issues. From those, the most common cause of ED overcrowding is the increase in arrivals of high acuity patients (Derlet *et al.*, 2001).
- Wait Time Targets: ED targets express the maximum amount of time that clinical evidence shows is appropriate to wait for a particular procedure (e.g., physician initial assessment or surgery wait time). These targets, which vary depending on the patient's severity level, are regulated in some communities. When a patient's wait time exceeds these thresholds, it implies ED overcrowding.
- Performance Metrics: Key performance indicators, often referred to as KPIs, or performance metrics are indicators of the effectiveness of ED operations and the quality of the services provided. Performance metrics are usually reported using average, $50^{th}$ percentile (median), or $90^{th}$ percentile estimates.
- Demand to Capacity Ratio (DCR): It is defined as the relationship between the actual patient arrival rate (pat./hour) and the maximum patient arrival that can be accommodated

by the ED based on its capacity. The DCR equals 1 when the ED reaches its maximum capacity. Thus, a DCR larger than 1.0 implies that critical services, such as emergency and operating rooms, are full and acceptable wait times have been exceeded.

### 2.1.3 Post-earthquake hospital functionality

Previous earthquakes such as those in Northridge (USA, 1994), Christchurch (New Zealand, 2011), and Illapel (Chile, 2015) have illustrated the impacts of reduced hospital functionality due to physical damage and the resulting health service deficit that occurs following a large earthquake. Consequently, hospitals have been recognized as post-disaster buildings in most building codes, such as NBCC 2015 (NRCC, 2015). The design intent is for these facilities to remain functional when a disaster, such as a major earthquake, occurs. In the code, this is implicitly achieved by increasing the design forces by an importance factor. However, this design intent is not explicitly verified. As shown in Figure 2.1, the loss of functionality in EDs after a disaster, and its impact on patient care, may occur as a result of physical damage to the facility (e.g., structural, nonstructural, and contents), the loss of critical hospital lifelines (e.g., water and electricity), discontinuities in different supply chains, or the reduction of critical personnel (Yavari *et al.*, 2010; Favier *et al.*, 2017).

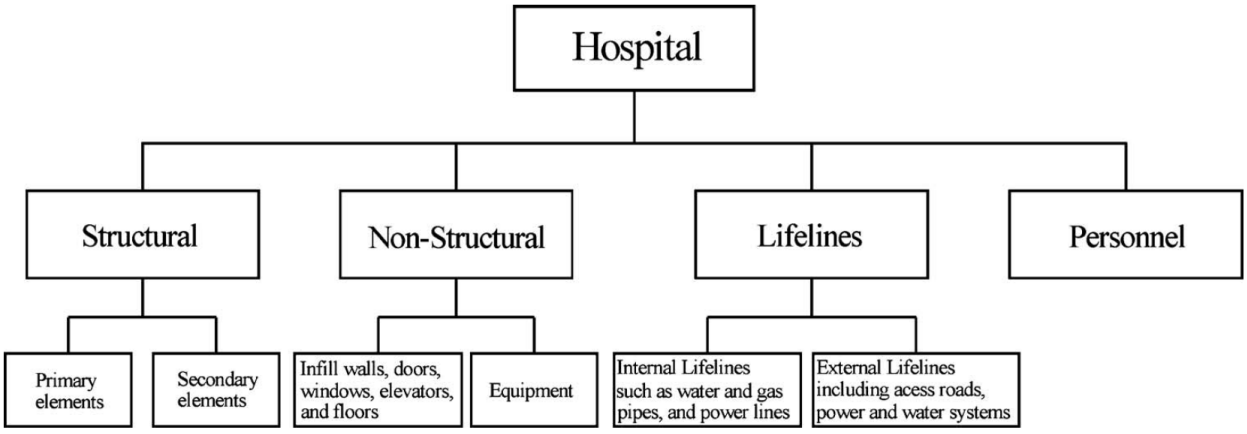


**Figure 2.1 Interacting systems influencing hospital functionality (Yavari *et al.*, 2010).**

Data on hospital performance in disasters is becoming increasingly available. Reconnaissance studies with a focus on the hospital post-earthquake functionality have been carried out following earthquakes in the United States, China, Haiti, New Zealand, Chile, and Ecuador (Schultz *et al.*, 2003; Wu *et al.*, 2008; Eberhard *et al.*, 2010; Jacques *et al.*, 2014; Mitrani-Reiser *et al.*, 2012, Vásquez *et al.*, 2017, Lanning *et al.*, 2016). Most of these studies not only include a detailed description of the hospital's overall performance, but also provide valuable information about the type of damage on structural and nonstructural components, lifelines outage, and the impact on hospital operations. Myrtle *et al.* (2005) conducted a comprehensive review of the performance of hospitals during several past earthquakes; and highlighted the importance of controlling the damage to piping systems, electrical, communication systems, medical monitors, HVAC, suspended ceilings, and fire sprinklers to maintain the functionality of a hospital following an earthquake. However, these studies did not explicitly link component damage to functionality loss of healthcare services.

Several authors have investigated the direct relationships between damage and loss of critical functions in hospitals. Holmes and Burkett (2006), based on historical data in California, suggested classifying structural and nonstructural damage into four levels: None, Minor, Affecting Hospital Operations, and Temporary Closure. Kuo, Banba, and Suzuki (2008) employed a probabilistic methodology to determine medical functionality loss in an earthquake. Their study accounted for damage to a limited number of non-structural components, however, did not account for damage to structural components or equipment. Lupoi *et al.* (2014) extended the component fragilities and introduced fault tree analysis to determine the functionality of different healthcare systems, including nonstructural, contents, and lifelines (e.g., power, water systems, etc.). However, the method did not account for interdependencies and did not quantify functionality.

Cimellaro, Reinhorn, and Bruneau (2010) developed a metamodel to estimate hospital capacity accounting for the influence of damage on both structural and nonstructural components by incorporating penalty factors. A single penalty factor was applied to the entire hospital and the study did not consider the distribution of damage throughout the building or the likelihood of damage to each healthcare unit or service area independently. Further, these methodologies did not consider the interdependencies between components.

By leveraging data from past earthquake observations, Yavari *et al.* (2010) defined four functionality classes for health care facilities: Fully Functional, Functional, Affected Functionality, and Not Functional (See Table 2.1). These functionality classes are determined from a decision tree diagram that accounts for the correlation between the Performance Levels of different systems: structural, non-structural, lifelines and staff. The performance level for each of the four major systems are based on the target performance levels established for healthcare buildings in FEMA 396 (FEMA, 2003); and they range from Performance Level 1 for no damage to Performance Level 4 for extensive damage. Yu *et al.* (2019) also adopted the four functionality levels shown in Table 2.1, and translated them to functionality percentages in order to quantify resilience; so, the functionality classes (from high to low) represented 100%, 50%, 30%, and 0% functionality of the healthcare facility. The causal dependencies between the failure of hospital systems and the functionality of relevant hospital services have also been represented using fault trees (Jacques *et al.*, 2014; Lupoi, Cavalieri, and Franchin, 2014). These methods could be used and adopted within the proposed framework. However, for the present study, the methodology by Yavari *et al.* (2010) was selected as it provides an explicit link between damage to structural and nonstructural components to different functionality classes considering interdependencies between systems. Another benefit of using this method is that it also provides component damage

descriptions that can be easily translated to damage states within the FEMA P-58 (FEMA, 2018) fragility database.

**Table 2.1 Functionality Classes for hospitals defined by Yavari *et al.* (2010).**

| Functionality Classes | Definition |
|---|---|
| Fully Functional | Service areas functionality is at normal levels |
| Functional | Functionality is lower than fully operational; however, none of the services areas was interrupted. |
| Affected Functionality | Some service areas are not able to provide normal services due to damage, but the facility is still able to provide some emergency services. |
| Not Functional | Facility is not functional and must be evacuated. |

### 2.1.4 Discrete event simulation of emergency departments

During a disaster condition, earthquake-induced patients increase the steady-state arrival of patients. This surge in demand, when coupled with an anticipated functionality loss of EDs, can result in the exceedance of the normal capacity of the ED and thus generate prolonged wait times which affect the quality of service. A powerful and versatile tool to investigate this problem is discrete event simulation (DES) modeling, which is introduced in this section. A literature review of the use of DES to evaluate the operations of EDs specifically during disaster conditions, such as an earthquake, is also presented.

Different modeling techniques have been proposed to analyze healthcare facilities, including discrete event simulation, agent-based simulation, and system dynamics. Referring back to Section 1.1, a computer simulation model able to accurately represent the dynamic behavior and strong queuing structure of an ED is desired. DES is the most popular and useful tool in this domain, as evidenced in a number of comprehensive reviews on ED simulation studies (Thorwarth and Arisha, 2009; Paul *et al.*, 2010; Gul and Guneri, 2015a). DES is capable of representing the micro-level behavior of EDs by modeling each patient as an entity with certain attributes that define its routing within the ED. DES models track and record the information of each patient from

the time of arrival (triage) to discharge; it thus provides performance metrics that can be used to evaluate ED operations. Further, DES is able to simulate "what if" scenarios, allowing the evaluation of possible emergency response plans or interventions. These strategies might include, for example, the deployment of field hospitals to temporally increase the number of resources (e.g., emergency rooms, beds, nurses, physicians), relocation of patients to a facility that is not badly impacted (i.e., ambulance diversion), among others. The ability to predict performance metrics for different scenarios allows DES to identify the most effective measure to deal with ED overcrowding when a disaster occurs.

Since 1980, DES has been used widely in the medical industry to study hospital response. The majority of these studies, however, focus primarily on evaluating the efficiency of certain ED resources and processes during 'normal' conditions without considering disaster surge scenarios (Morton *et al.*, 2015). A comprehensive literature review of DES studies (Gul and Guneri, 2015a) suggests that the use of this modeling technique to simulate disaster situations has been gaining interest since 2010. For instance, Joshi and Rys (2011), Xiao *et al.* (2012), and Lin *et al.* (2015) have developed models to optimize the ED workflow by considering a patient surge during extreme events. However, the methods did not account for disaster-related injuries, but instead, different arrival rates in quantity and pattern due to hypothetical catastrophic events were assumed. More recent studies have improved the feasibility of the simulation by leveraging hospital data following a disaster.

For earthquake disaster situations specifically, Yi *et al.* (2010), Gul *et al.* (2020), Yu *et al.* (2020), Lin *et al.* (2021), and Fava *et al.* (2021) have utilized DES models to analyze the hospital EDs behavior during plausible earthquake scenarios in Turkey, China, Taiwan, and Italy. Researchers have proposed different approaches to build a versatile and generic model able to

analyze ED surge capacity and be scalable to analyze hospital networks instead of individual EDs. The main inputs to build such models are the patient routing definition, and the actual data of ED operations to determine wait times and capacities of each service area to be considered. This ED data can be gathered via personal communication with management staff, surveys, interviews, on-site observations, among other methods. An important aspect in ED simulation that has improved in recent years, is how to appropriately model and estimate the arrival rate of patients, a key input data to a DES model. For instance, Cimellaro *et al.* (2010), used the pattern of arrival rates of patients in the aftermath of the 1994 Northridge earthquake (USA) and scaled it according to the seismic hazard at the location of the ED analyzed. By using the same logic, Yu *et al.* (2020) leveraged the data collected during the 2008 Wenchuan earthquake (China) and amplified the seismic arrival input to study the impact of earthquake magnitude on the ED performance metrics. Lin *et al.* (2021) adopted the same approach and used multiplicative scale factors ranging from 1.4 to 2.3 times the normal arrival rate, to amplify the input data of the DES model, and analyze the sensitivity of the ED operations.

While the abovementioned DES models provide valuable information for disaster preparedness management, one of the major limitations is that they did not account for the ED capacity reduction due to the anticipated damage and consequent functionality loss after a major earthquake. This is an important factor to consider when evaluating ED surge capacity because the loss of functionality might have a greater impact than the surge in demand on the overall ED performance. The contribution of each of these factors on the ED performance metrics will depend primarily on the earthquake intensity level, the seismic performance of the hospital and the damage to buildings (and associated injuries) in the catchment area served by the hospital. To address this research gap, limited studies attempted to explicitly consider capacity loss due to damage. As such,

Cimellaro, Reinhorn, and Bruneau (2010) incorporated the influence of physical damage by applying single penalty factors for the complete hospital to their original methodology. The framework aimed to assess more accurately the seismic resilience of hospitals using DES and metamodels, but it did not consider the damage at the building component level or the likelihood of damage to each healthcare unit or service area independently. This method was implemented in different case studies including a single ED in Italy, and a hospital network in the USA (Cimellaro *et al.*, 2016). Poulos *et al.* (2015) performed a scenario-based assessment using DES and quantified the contribution of each factor (i.e., loss of functionality and increase of healthcare demand) to the daily waiting time in an earthquake scenario. Favier *et al.* (2019) developed an intensity-based seismic risk assessment framework using DES that accounted for ED functionality loss of critical ED services areas (i.e., emergency rooms and operating rooms). Nevertheless, these scenario and intensity-based assessments did not capture the inherent variability of the demand estimation (i.e., earthquake-induced arrivals), and the functionality loss calculation only accounted for damage to a limited number of nonstructural components (ceilings, partition walls, and doors).

In the present thesis, DES modeling is incorporated into a seismic risk assessment framework to simulate ED operations following a damaging earthquake. Different scenarios are analyzed to evaluate the functionality loss due to seismic damage in structural and nonstructural building components of the hospital facility, as well as a variable surge in demand dependent on a multi-severity casualty estimation. To implement this methodology, in addition to the input data listed earlier to build a DES model, a seismic fragility study of the hospital ED building is required. A simplified structural model is used to estimate the component damage and the associated functionality loss of ED services. These results can then be leveraged to update the ED service

area capacities in the DES model, and thus simulate the impact of the earthquake in the ED operations.

## 2.2 Seismic damage simulation of buildings

The objective of this section is to present available structural analysis models to estimate the seismic damage of buildings. An accurate and rapid assessment of seismic damage, and post-event repair time can provide valuable input for emergency response and post-earthquake recovery (Lu *et al.*, 2019). Therefore, it is crucial to develop a robust earthquake damage prediction model suitable for hospitals, and the buildings in the catchment area served by the hospital.

In this context, HAZUS (FEMA, 2020) developed a method suitable for estimating earthquake damage to buildings at a regional level. The model evaluates the distribution of building damage states by utilizing fragility functions that relate the ground motion intensity (i.e., Sa(T) or PGA) to the building structural damage. The building models used to derive these functions consist of SDOF systems, hence, the resulting fragility curves are based on their first mode of vibration. The resulting damage of the SDOF model represents the overall damage of the buildings but does not provide damage estimates on a floor basis.

While the HAZUS methodology is widely accepted to conduct seismic damage assessments at a regional and national level, it employs single-degree-of-freedom (SDOF) models, and thus it is not able to represent the damage distribution results at a floor level of detail. In this context, the Federal Emergency Management Agency (FEMA) came up with the FEMA P-58 report (FEMA, 2018) which defines the objective and procedure of next-generation performance-based seismic design. FEMA P-58 (FEMA, 2018) proposes a component-level damage assessment methodology that accounts for the fragility of every structural and nonstructural component in a building. To implement the FEMA P-58 method, a detailed seismic response of the building (i.e.,

engineering demand parameters, or EDPs) is required, as well as the structural and nonstructural component data, which includes their quantities and distribution throughout the building.

In this study, one of the objectives is to explicitly account for the functionality loss of the ED services areas on each floor due to the structural and non-structural damage; therefore, it is vital to estimate the damage at the component level of the building. Thus, a structural model capable of providing a rapid estimate of the Engineering Demand Parameters (EDPs) in each floor of a building is desirable for the analysis of the hospital buildings.

### 2.2.1 Scenario damage assessment using SDOF models / Low-fidelity models

Currently, the most well-known tool for risk and damage simulation for earthquake disaster prevention and mitigation is HAZUS, developed by the Federal Emergency Management Agency (FEMA, 2020). The method requires knowledge of the building taxonomy and an estimate of the level of ground shaking as an input. The method proposes 36 typical building types considering their material, lateral force-resisting system, and height range. This information, together with the design level (i.e., high-code, moderate-code, low-code, pre-code buildings) and occupancy (e.g., residential, office, healthcare) are used to assign an appropriate taxonomy to every building. To estimate building damage, the method utilizes fragility curves that describe the probability of observing different damage states (i.e., no damage, slight, extensive, and complete damage state) for a given ground shaking intensity measure. Three ground motion shaking intensity measures, expressed in terms of spectral acceleration ($SA$) at building periods ($T$) of $0.3s$, $0.6s$, and $1.0s$ for low-rise, mid-rise, and high-rise buildings, respectively are used. These building periods encompass the fragility data available for the HAZUS building taxonomies.

Following the framework of HAZUS (FEMA, 2020), researchers have developed computer simulation programs such as OpenQuake (GEM, 2021), which provide a scenario damage

assessment module. This tool allows the users to perform the calculation of damage distribution statistics in a portfolio of buildings subjected to different earthquake scenarios while accounting for the uncertainties of the ground shaking. The module requires knowledge of the exposure model, relevant fragility functions for each building in the exposure file, and ground motion fields as needed for the different fragility functions. The exposure primarily contains data on the spatial distribution of the building inventory. Building taxonomies are used to link the assets in the region to the relevant fragility functions. Ground motion fields are computed for each building at the relevant site and for the corresponding intensity measure in accordance with the fragility functions. As a result, the probability damage state distribution of every building in the exposure is obtained. Further, consequence models can also be provided as inputs for the scenario damage calculation. These models are utilized to estimate, for example, earthquake-induced injuries or direct economic losses, based on the calculated damage distribution.

The present method is suitable and reliable as a predictor of damage for large population groups (i.e., regional level); however, it is not recommended for predicting damage to a specific facility (FEMA, 2020). Some of the limitations of this method are as follows: (1) it does not account for the contribution of higher mode effect to structural response, (2) it is not able to capture certain ground motion characteristics, such as duration or velocity pulses, and (3) it is not able to explicitly estimate damage on a story basis. The FEMA P-58 methodology (FEMA, 2018) provides a solution for the above limitations of the HAZUS method. As mentioned before, the FEMA P-58 method requires a detailed seismic response of the building (i.e., EDPs). Thus, researchers have proposed nonlinear multiple degree-of-freedom (MDOF) models in conjunction with time-history analysis to predict seismic damage to buildings.

### 2.2.2 Computational/Numerical models

Earthquake-induced component damage is calculated from EDPs, including story drift ratio and floor acceleration for each floor. While refined nonlinear finite element (FE) models are used to accurately simulate EDPs, these detailed models are impractical for regional seismic simulations due to the limited availability of building information and high computational requirements. Therefore, it is critical to establish numerical models that rely on easily accessible data and can accurately stimulate the seismic response of buildings of different characteristics (e.g., lateral force-resisting system, height, etc.) to be used on a regional scale. Simplified multi-degree-of-freedom (MDOF) models have been proposed to overcome this limitation. The accuracy and efficiency of simplified MDOF models in predicting EDPs have been demonstrated in previous studies (Taghavi and Miranda, 2005; Lu *et al.*, 2014; Xiong *et al.*, 2016; Kuang and Huang, 2011), making these models suitable for damage prediction on a regional scale.

Lu *et al.* (2014) developed non-linear MDOF shear (NMS) model able to predict the seismic response of buildings through nonlinear time history analysis. This method, which has been adopted by NHERI (NHERI SimCenter, 2018) through the 'MDOF-LU' application tool, utilizes HAZUS data to generate numerical models based on widely accessible building attribute data (i.e., number of stories, year of construction, occupancy, geometry, structural system). The NMS model consists of a multi-story non-linear shear column with lumped masses, so it is appropriate for those structures in which shear failure is most significant (e.g., moment frame systems). The method can provide the seismic response of each story, and thus its resolution is much better than that of an SDOF model that provides a single response metric for the entire building. However, the NMS model fails to accurately simulate shear wall systems and tall

buildings, where the flexural component governs the deformations. Hence, this model is only appropriate for urban areas where most of the buildings are mid-rise or low-rise.

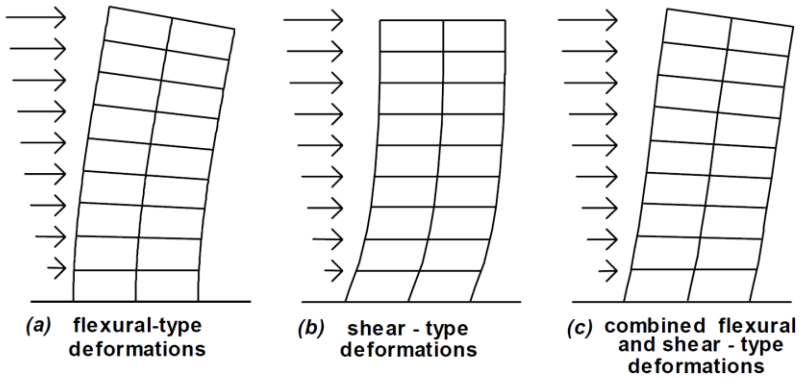


**Figure 2.2 Overall lateral deformations in multistory buildings (Taghavi and Miranda, 2004).**

Figure 2.2 illustrates the influence of shear and flexural deformation on a building. The global flexural deformation of tall buildings plays an important role in the seismic deformation modes of these structures. Given the importance of tall buildings in modern urban areas (widely used for residential buildings, offices, hospitals, etc.), models capable of representing both inter-story shear and flexural deformations are required. In this context, Xiong *et al.* (2016) proposed a non-linear MDOF flexural shear (NMFS) model. This model accounts for the influence of high-order vibration modes and can accurately represent the nonlinear flexural-shear deformation mode of buildings, making it suitable to simulate a wide array of lateral systems of different heights. Once the EDPs at each building floor are accurately predicted, a component-level damage assessment can be performed, for instance, following the FEMA P-58 methodology (FEMA, 2018).

### 2.2.3 Nonlinear MDOF flexural-shear (NMFS) model – Moderate fidelity models

In the NMFS model proposed by (Xiong *et al.*, 2016), the flexural deformation and shear deformation of buildings are simulated using a nonlinear flexural spring and a nonlinear shear spring per story connected by rigid links. Figure 2.3 shows the general configuration of an NMFS

model, where the mass per floor is lumped at the nodes. The properties of the flexural and shear springs are regulated by the properties of the shear wall and frame system, respectively.

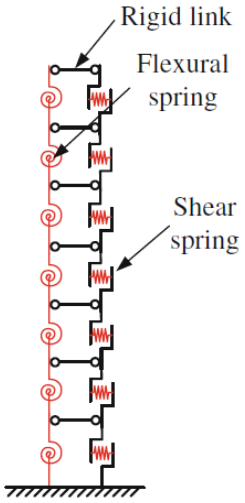


**Figure 2.3 Nonlinear MDOF flexural-shear (NMFS) model (Xiong *et al.*, 2016).**

The advantages of the NMFS model include:

a. It can accurately represent the nonlinear flexural-shear deformation mode of buildings; this makes the model suitable to represent both moment frame and shear wall systems.
b. It has high computational efficiency in comparison with refined FE models.
c. Its parameter calibration is easy to implement. If detailed information is not available, the HAZUS method (FEMA, 2020) can be used to define the necessary input parameters.
d. It is capable of calculating the EDPs of each building story.

**Parameter calibration based on building attribute data.**

The NMFS model utilizes tri-linear backbone curves to simulate the nonlinear behavior of different stories. Figure 2.4 presents the tri-linear curves for both shear and flexural springs and the main parameters that define the three control points of the tri-linear backbone curve: yield, peak, and ultimate strength. The parameter calibration follows the procedure described by Xiong *et al.*

(2016), and it is primarily based on the widely accessible building attribute data (i.e., number of stories, year of construction, occupancy, geometry, structural system).

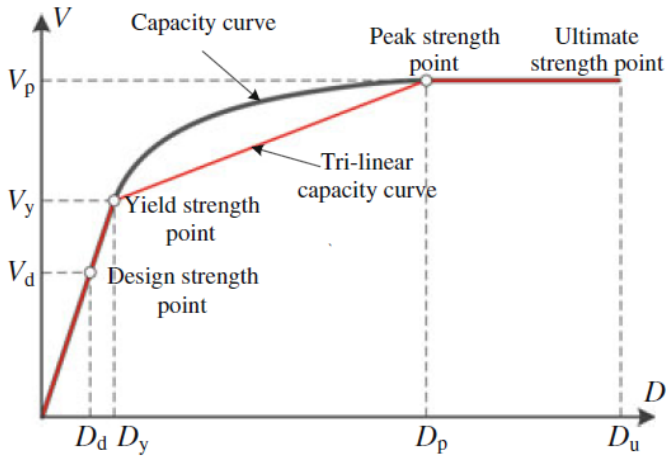


**Figure 2.4 Trilinear backbone curve suggested by HAZUS (FEMA 2012c).**

The procedure to develop the simplified NMFS model for estimation of seismic response (with emphasis on RC frame shear wall dual system structures) is presented in the following step-by-step form:

**Step 1.** Collect the building attribute data:

Based on this information and additional design details, estimate the seismic mass and height of each story. If such data is not available, a HAZUS consistent building taxonomy (structural type, code level, occupancy) can be used to define the necessary input parameters.

**Step 2.** Calibration of elastic parameters:

Based on the building attribute data (height, and structural type) the first, $T_1$, and second, $T_2$, periods of vibration are estimated using empirical equations. For example, the first period of an RC shear wall structure can be determined using the empirical period formula recommended by the NBCC 2015 (NRCC, 2015), as shown in Eq. 2.1. The second period can be calculated using the widely adopted empirical relationship given in Eq. 2.2 (Lagomarsino 1993).

$$T_1 = 0.05(H)^{3/4} \quad (2.1)$$

$$T_2 = 0.27\,T_1 \quad (2.2)$$

where $H$ is the total height of the building. After obtaining the relevant periods of vibration, estimates of the flexural stiffness, $EI$, and shear stiffness, $GA$, both assumed to be constant at the building height, can be obtained as a function of $T_1$ and $T_2$ following the methodology outlined by Taghavi and Miranda (2005). By performing modal analysis of the simplified analysis model, the stiffnesses can be adjusted to the relevant periods of vibration.

**Step 3.** Calibration of yield point:

The design base shear, $V_d$ and bending moment, $M_d$ are initially estimated based on nominal design strengths required by the corresponding building code (determined from the year of construction, and assuming that the design adhered to the corresponding code edition). The design shear coefficient, $C_s$ as defined in most standards (e.g., NBCC 2015, ASCE 7-16) can also be used. This parameter represents the base shear, $V_d$ as a fraction of the total seismic mass of a building. The design shear coefficient, $C_s$ can also be obtained from Table 5.4 of HAZUS (FEMA, 2020) if detailed building data is not available. After obtaining the design shear and bending moment, the yield strength at the base, $V_{y,1}$ and $M_{y,1}$ can be derived as follows:

$$V_{y,1} = V_d\,\Omega_\gamma \quad (2.3)$$

$$M_{y,1} = M_d\,\Omega_\gamma \quad (2.4)$$

where $\Omega_\gamma$ is the overstrength factor relating "true" yield strength to design strength, and can be obtained from Table 5.4 of HAZUS (FEMA, 2020), or engineering judgment. Once the base shear and flexural yielding capacity, $V_{y,1}$ and $M_{y,1}$ respectively, are estimated, the story yield shear and flexural strength, $V_{y,i}$ and $M_{y,i}$ can be obtained as follows:

$$V_{y,i} = V_{y,1}\left(1 - \frac{i(i-1)}{n(n+1)}\right) \quad (2.5)$$

$$M_{y,i} = M_{y,1}\left(1 - \frac{0.6(i-1)}{n-1}\right) \quad (2.6)$$

where $i$ is an index indicating the floor number, and $n$ is the number of floors. Eq. 2.5 is derived considering that all floors have the same mass and height, and thus the inter-story shear strengths of each story and the sum of lateral load of the above stories can be considered as a linear relationship. Eq 2.6 is derived considering that the moment strength variation along the height is approximately linear, decreasing from the base level to the roof. In this case, the yield moment at the roof is assumed to be 40% of the base moment. Finally, the corresponding yield displacement, $\Delta u_{y,i}$ and rotation, $\Delta\theta_{y,i}$ are determined according to:

$$\Delta u_{y,i} = \frac{V_{y,i}\, h_i}{GA} \quad (2.7)$$

$$\Delta\theta_{y,i} = \frac{M_{y,i}\, h_i}{EI} \quad (2.8)$$

**Step 4.** Calibration of peak point:

The peak shear strength, $V_{p,i}$ and bending strength, $V_{p,i}$, as well as the peak displacement, $\Delta u_{p,i}$ and rotation, $\Delta\theta_{p,i}$ are determined as follows:

$$V_{p,i} = V_{y,i}\, \Omega_p \quad (2.9)$$

$$M_{p,i} = M_{y,i}\, \Omega_p \quad (2.10)$$

$$\Delta u_{p,i} = \mu\, \Delta u_{y,i} \quad (2.11)$$

$$\Delta\theta_{p,i} = \mu\, \Delta\theta_{y,i} \quad (2.12)$$

where $\Omega_p$ is the overstrength factor, and $\mu$ is the ductility factor that relates the yield and peak displacements. These parameters can be obtained from Tables 5.5 and 5.6 of HAZUS (FEMA,

2020), respectively. These parameters vary for different types of structures and can also be obtained from the corresponding building code or engineering judgment. Alternatively, the stiffness reduction factor, $\eta$ can be used to determine the peak displacements $\Delta u_{p,i}$ and rotation, $\Delta\theta_{p,i}$ by using Eq. 2.14 and 2.15. For concrete buildings, the stiffness reduction factor, $\eta$ can be determined according to Provision 6.6.3.1.1 of ACI 318 (2014).

$$\Delta u_{p,i} = \frac{V_{p,i}\, h_i}{\eta\, GA} \tag{2.13}$$

$$\Delta\theta_{p,i} = \frac{M_{p,i}\, h_i}{\eta\, EI} \tag{2.14}$$

**Step 5.** Ultimate strength point:

The ultimate strength, $V_{u,i}$ and $M_{u,i}$ equals the peak strength. The ultimate displacement/rotation, $\Delta\theta_{u,i}$ and $\Delta u_{u,i}$ can be derived from the inter-story drift threshold at the complete damage state, $\delta_{complete.DS}$ as per Tables 5.9a, 5.9b, and 5.9c of HAZUS (FEMA, 2020).

$$V_{u,i} = V_{p,i} \tag{2.15}$$

$$M_{u,i} = M_{u,i} \tag{2.16}$$

$$\Delta\theta_{u,i} = \delta_{complete.DS} \tag{2.17}$$

$$\Delta u_{u,i} = \Delta\theta_{p,i}\, h_i \tag{2.18}$$

**Step 6.** Hysteretic parameter calibration:

For the convenience of the calibration process, the single-parameter hysteretic model proposed by (Steelman and Hajjar, 2009) is adopted, in which only one parameter τ must be determined. This parameter is defined as the ratio between the areas enclosed by the pinching envelope and that under the full bi-linear envelope. As such, this parameter quantifies the severity of degradation, and so it can be related to the degradation factor as per Table 5.18 of HAZUS (FEMA, 2020) which

is a function of the earthquake intensity level and building type. This single parameter-pinching model has been validated for RC frame-shear wall structures, and it is recommended for conventional buildings with regular planar and vertical layouts (Xiong *et al.*, 2016). Other pinching models (e.g., Ibarra *et al.*, 2005) can be used; however, more parameters might need to be calibrated.

In Appendix A, an application of the procedure is demonstrated for a 12-story RC shear wall building. Further, the model is validated via a comparison study against a refined FE model developed by Marafi *et al.*, 2019. To demonstrate the accuracy and computational efficiency of the NMFS model, both models are subjected to 30 $M_w$9.0 CSZ earthquake scenarios, and the resulting EDPs from the nonlinear time-history analysis are compared.

# Chapter 3: Methodology

## 3.1 Overview

The steps of the proposed methodology to evaluate the post-earthquake functionality and surge capacity of emergency departments (EDs) are summarized in Figure 3.1. The methodology consists of four phases: (1) seismic hazard, (2) hospital demand, (3) hospital functionality loss, and (4) post-earthquake surge capacity. In Phase 1, *N* scenario-based ground motion simulations are generated to obtain ground motion intensity maps for Phase 2 and consistent acceleration time histories for Phase 3. In Phase 2, a multi-severity casualty estimation is performed following the methodology presented in HAZUS (FEMA, 2020) to estimate patient surge. In Phase 3, the ED capacity to treat patients immediately after the earthquake is estimated with explicit consideration of structural and nonstructural component damage in the hospital building. Phase 3 involves three steps:

- Step A: Perform a nonlinear response history analysis using a simplified non-linear structural model of the hospital structure.
- Step B: Assess the physical damage to the building with the Engineering Demand Parameters (EDPs) from Step A using the FEMA P-58 methodology (FEMA, 2018).
- Step C: Determine the functionality loss and assign a Performance Level to each floor of the hospital to link structural and non-structural damage to the post-earthquake functionality of service areas within the ED.

Lastly, in Phase 4, a DES model is used to simulate patient flow within the emergency department to determine the surge capacity. To account for the uncertainties related to casualty modeling (required to estimate the healthcare demand), and the vulnerability of building components to

seismic damage (required to estimate the reduction in hospital capacity), $K_D$ and $K_C$ Monte Carlo realizations are performed, respectively. The simulation results provide relevant ED performance metrics such as wait time and length of stay for patients with injuries of different severity for each earthquake scenario. This methodology is also used in a case study to quantify the improvement in hospital performance when mitigation measures are implemented to relieve ED crowding, demonstrating the value in supporting planning by health authorities and emergency response teams.

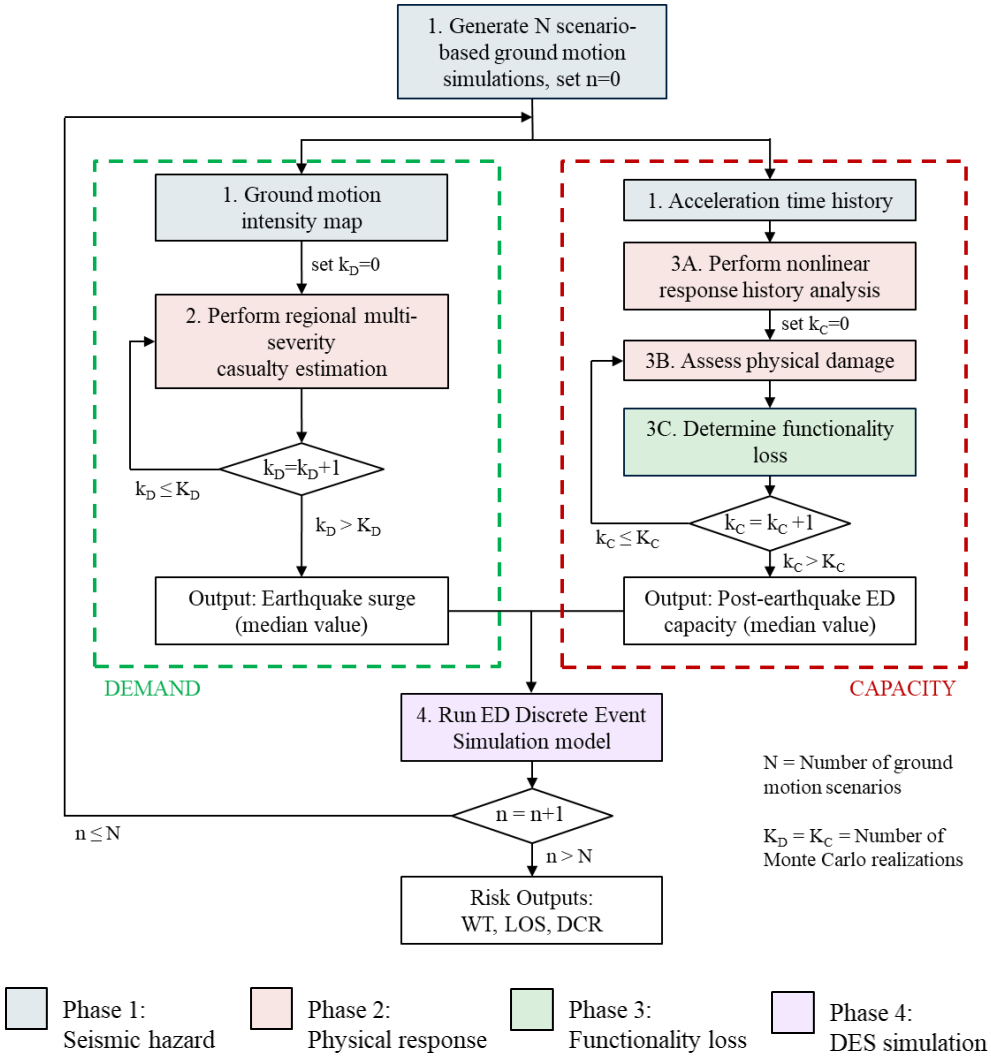


**Figure 3.1 Methodology to quantify the post-earthquake functionality and surge capacity of a hospital emergency department.**

## 3.2 Seismic hazard analysis

A deterministic scenario-based assessment is used to characterize the seismic hazard. A set of *N* physics-based ground motion simulations (e.g., Frankel *et al.*, 2018) are used to estimate ground motion shaking across the entire region of interest. As shown in Figure 3.1, using physics-based simulations permits the generation of consistent (1) ground motion intensity maps for a regional seismic risk assessment to estimate casualties and (2) acceleration time histories for a detailed functionality loss assessment of the hospital building.

To estimate demand, the exposure model of the catchment area of the hospital is required. The exposure model includes the spatial distribution of the building stock along with the structural characteristics (e.g., construction age, material, height, lateral resisting system type) and the population model of each building. The population model describes the temporal variation (e.g., day vs night) of building occupants for different occupancy types (e.g., residential vs commercial). The HAZUS methodology (FEMA, 2020) presented in Section 2.2.2, and implemented within the OpenQuake engine (GEM, 2021) is used to perform a regional seismic risk assessment. Damage to buildings is estimated by means of fragility functions, which describe the conditional probability of observing different damage states as a function of a ground motion intensity measure. Ground motion intensity maps are thus generated for the intensity measures of the fragility functions within the exposure model. Consequence functions are then used to translate damage to casualty estimates using the population model.

To estimate capacity, the simplified NMFS model presented in Section 2.2.3 to simulate the seismic response of the hospital buildings. *N* acceleration time histories are generated to simulate the nonlinear response of the relevant hospital buildings. The engineering demand

parameters (EDPs) predicted from the nonlinear time-history analysis are used to conduct the functionality loss of the service areas within each floor of the buildings of interest.

### 3.3 Post-earthquake surge estimation

In recent decades, EDs have suffered from frequent crowding under normal conditions, with more than 90% of EDs in the United States reporting overcrowding as a problem (Derlet, Richards, and Richard, 2001). Extreme natural events can significantly exacerbate the situation due to large surges in casualty arrivals. In this study, the post-earthquake surge in patient arrivals due to regional casualties is determined using multi-severity casualty estimation. Only casualties directly caused by building damage (structural and non-structural) are considered since this is the controlling factor for injuries and fatalities during an earthquake (Spence *et al.*, 2011). The spatial distribution of injuries with varying levels of severity ranging from immediate death to minor injuries is obtained by employing the HAZUS methodology (FEMA, 2020), as explained in Section 2.2.1. Alternatively, other analytical models can be employed for casualty estimation, such as the model developed by Ceferino *et al.* (2018a). This probabilistic approach extends the PBEE framework to multiple-building analysis, enabling the calculation of the joint probability distribution of multi-severity casualties, including spatial and across-severity correlations. An application of this method can be found in Ceferino *et al.* (2018b).

In this study, the exposure model is defined based on the proximity to the hospital and the estimated population served by the ED of interest. Using ground motion intensity maps generated in Phase 1, a regional building damage assessment is performed using OpenQuake (GEM, 2021). To account for the inherent uncertainty in ground motion shaking, $K_D$ possible realizations are sampled for each earthquake scenario. Damage to the built environment and its variability is estimated via physics-based fragilities that capture salient building features. As a result, the

damage state probability distribution of each building in the exposure model is determined, ranging from no damage to complete damage/collapse. Finally, the indoor and outdoor casualties are determined by linking the seismic damage states with the associated consequence functions from HAZUS (FEMA, 2020). These functions account for the casualties caused by both structural and non-structural damage, although non-structural casualties are not directly derived from non-structural damage but instead are derived from structural damage output. The variation in the spatial distribution of the population over time is also captured by considering the different times of occurrence of the earthquake (i.e., day, transit, and night). The assessment does not include potential casualties from non-building-related failures.

**Table 3.1 Injury severity level description (FEMA, 2020).**

| Injury Severity Level | Injury Description |
|---|---|
| Severity 1 | Injuries requiring basic medical aid that could be administered by paraprofessionals. These types of injuries would require bandages or observation. Some examples are: a sprain, a severe cut requiring stitches, a minor burn (first degree or second degree on a small part of the body), or a bump on the head without loss of consciousness. Injuries of lesser severity that could be self treated are not estimated by Hazus. |
| Severity 2 | Injuries requiring a greater degree of medical care and use of medical technology such as x-rays or surgery, but not expected to progress to a life threatening status. Some examples are third degree burns or second degree burns over large parts of the body, a bump on the head that causes loss of consciousness, fractured bone, dehydration or exposure. |
| Severity 3 | Injuries that pose an immediate life threatening condition if not treated adequately and expeditiously. Some examples are: uncontrolled bleeding, punctured organ, other internal injuries, spinal column injuries, or crush syndrome. |
| Severity 4 | Instantaneously killed or mortally injured |

Injuries are categorized into four severity levels according to Table 3.1 based on HAZUS (FEMA, 2020). These severity levels, excluding Severity 4 which corresponds to instantaneous death, are translated into the three different color codes for patients: red, yellow, and green. This classification system is based on the widely implemented Simple Triage and Rapid Treatment method (Benson *et al.*, 1996) which is suitable for emergency patient triage during a mass casualty

incident such as a catastrophic earthquake. Patients with Severity Level 3 injuries (e.g., having uncontrolled bleeding or punctured organs) are classified as Red codes (Emergency). Likewise, patients with Severity Level 2 injuries (e.g., fractured bone, or a bump on the head that causes loss of consciousness), are classified as Yellow codes (Urgency). Lastly, Severity Level 1 patients who have no acute symptoms and need relatively few resources to complete treatments are classified as Green Codes (Minor Urgency). Hereinafter, color coding is used to refer to patient acuity.

After estimating the number of injured people, the arrival pattern and time duration in which patients arrive at the ED after the earthquake are defined using empirical or numerical methods. Empirical methods consist of scaling arrival rate curves from previous earthquakes (e.g., Cimellaro, Reinhorn, and Bruneau, 2010; Pianigiani *et al.*, 2014). However, such curves are not easily available for many regions and also cannot capture the spatial distribution of damage from different earthquake scenarios or changes to the community such as the demographic changes. Another option is using a simplified numerical model that estimates the earthquake-induced patient arrival based on mathematical equations (e.g., Fawcett and Oliveira, 2000). However, these methods do not represent the physics of the hazard and response and do not capture the wide range of inherent variability. Regardless of the method selected, the patient arrival rate must follow a non-stationary exponential distribution (Gross *et al.*, 2008) with a variable arrival rate parameter obtained from the estimated average hourly arrival rate. Based on observations from past earthquakes, these arrivals might occur up to 2-4 days after an earthquake (Yi, 2005; Ceferino *et al.*, 2020).

### 3.4 Modeling emergency department functionality

The loss of functionality in EDs after a disaster, and its impact on patient care, may occur as a result of physical damage to the facility (e.g., structural, nonstructural, and contents), the loss of

critical hospital lifelines (e.g., water and electricity), discontinuities in different supply chains, or the reduction of critical personnel (Favier *et al.*, 2017). In this section, the loss of functionality due to the damage of structural and non-structural building components (Phase 3, Steps A to C) is investigated.

### 3.4.1 Structural response simulation

In this study, a nonlinear MDOF flexural-shear (NMFS) model of the hospital structure is developed following the methodology developed by Xiong *et al.* (2016). The advantage of NMFS models is that they accurately represent the nonlinear flexural-shear deformation mode of buildings, making it suitable to simulate a wide array of lateral systems, including both moment frame and shear wall systems. Further, as explained in Section 2.2.3, NMFS models are easy to calibrate and are computationally efficient compared to a refined FE model (Lu *et al.*, 2019). A two-dimensional (2D) model is built for each direction of the structure and the EDPs are determined from response-history analysis. Orthogonal directions are uncoupled, and torsion effects are not considered in the analysis model. The simulation is performed using OpenSeesPy, a Python library for the OpenSees finite element framework (Zhu *et al.*, 2018). The nonlinear flexural spring and shear spring are modeled together in a 'TwoNodeLink' element as shown in Figure 3.2 (a). The properties of the flexural and shear springs are assigned to the rotational and transverse response of the element, respectively. An infinitely rigid element is assigned to the axial spring. One element per story is modeled with the mass lumped at the story nodes.

The parameter calibration method requires at minimum the following building attributes: structural height, year of construction, material, and structural system design. These building attributes are used to assign a HAZUS taxonomy and the code level design. Calibration parameters including the period of vibration, design shear coefficient, overstrength factor, ductility,

degradation factor, are obtained from Tables 5.4, 5.5, 5.6, and 5.18 of the HAZUS Technical Report (FEMA, 2020). Detailed building data (e.g., design drawings) can be used to refine the associated MDOF system properties (e.g., base shear, moment strength, fundamental periods, ductility, etc.). The details of the procedure used to develop the simplified NMFS models to estimate the seismic response of RC shear wall and moment frame buildings are provided in Section 2.2.3.

To validate the accuracy and computational efficiency of the NMFS model, the response of a 12-story RC shear wall building subjected to 30 ground motion simulations of an $M_w$9.0 CSZ earthquake scenario in Seattle, Washington is studied. This structure and location are selected for calibration because a high level of nonlinearity in the structure is expected, and the lateral system is consistent with that of the case study hospital building presented later. The seismic response (i.e., periods of vibration, pushover curve, story shears, story drifts) from the simplified NMFS model are compared with those of a refined FE model developed by Marafi *et al.* (2019). As seen in Figure 3.2 (b), the refined model consists of a solid wall and utilizes six displacement-based beam-column elements (DBE) per story, with five integration points per element. Shear deformations were modeled using a linear elastic shear spring per element. Both models are implemented using OpenSees. The mean story drift ratios and floor accelerations determined using the simplified model are consistent with those of the refined model as observed in Figures 3.2 (b) and 3.2 (c). A detailed description of the parameter calibration procedure and the validation of the NMFS model is provided in Appendix A.

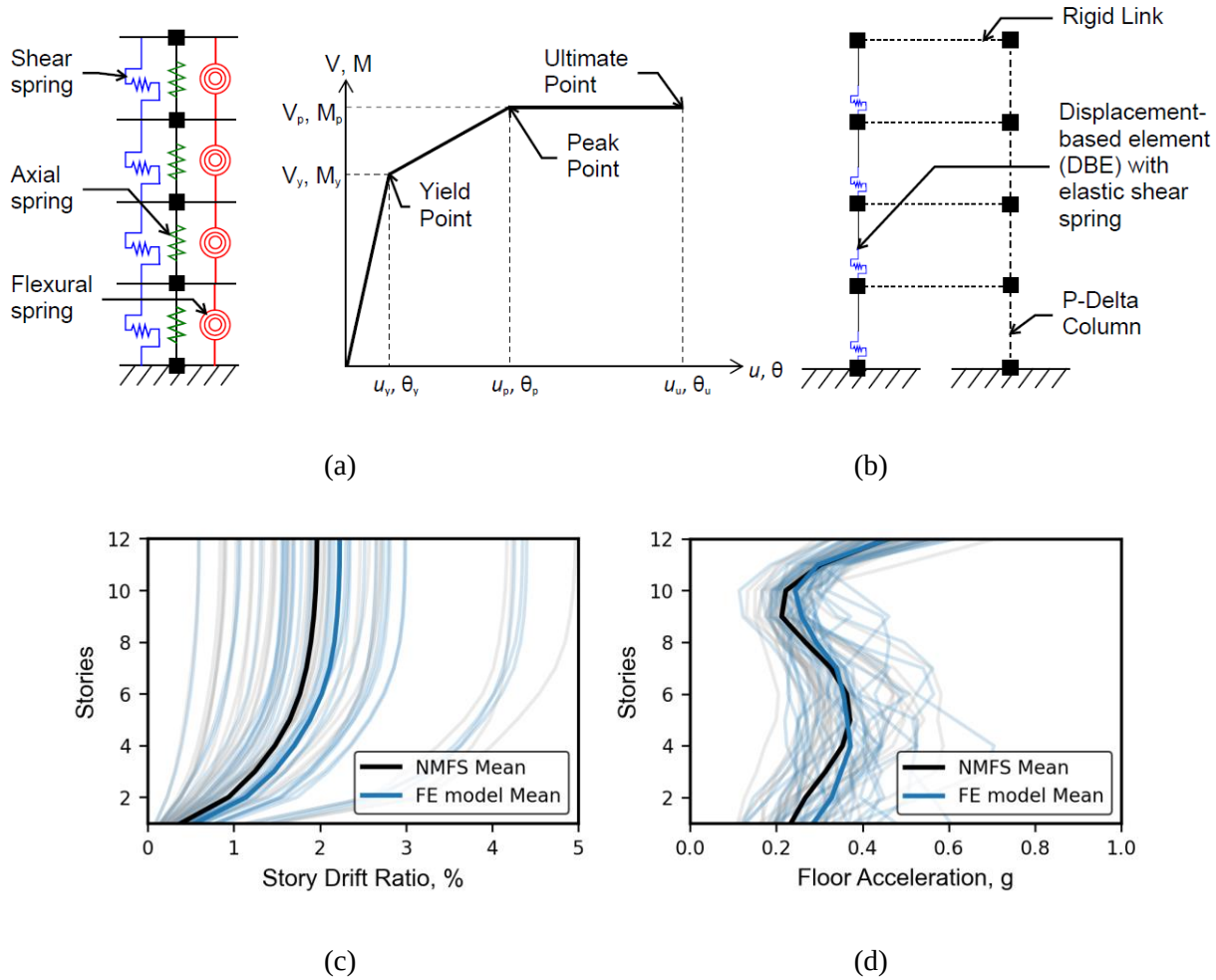


**Figure 3.2 Validation of the simplified nonlinear model: (a) NMFS analytical model, (b) FE refined model, (c) story drift ratio, and (d) floor acceleration results of a 12-story RC shear wall building subjected to 30 simulated ground motions of an Mw9.0 CSZ earthquake in Seattle, WA.**

### 3.4.2 Building performance assessment

To assess the damage to structural and non-structural components of the ED, a building performance model of the hospital is created following the FEMA P-58 methodology (FEMA, 2018). FEMA P-58 relates EDPs (e.g., story drift ratios and floor accelerations) to damage of individual building components (e.g., concrete walls, architectural glazing, water piping, etc.). The damage assessment is performed using NHERI-SimCenter's Pelicun (Zsarnoczay and Kourehpaz,

2021), a python package that implements the FEMA P-58 methodology. Structural component quantities are determined from the structural drawings of the building. Non-structural component quantities are estimated based on typical quantities found in health care facilities using the FEMA P-58 Normative Quantity Estimation Tool (FEMA, 2018) and are adjusted if additional site-specific data is available. The components considered for hospital buildings include suspended ceilings, partition walls, curtain walls, elevators, and hot- and cold-water piping. For each of the $N$ scenario-based ground motion simulations, $N$ sets of EDPs are calculated. From each set of EDPs, $K_C$ Monte Carlo realizations (usually 1,000) are performed for the hospital building to propagate uncertainties through the damage assessment framework. For each realization, the building damage data is obtained, and the associated functionality loss is determined as described next.

### 3.4.3 Functionality loss assessment

Several studies have investigated the post-earthquake functionality of health care facilities (see Section 2.1.3). In this study, a method to estimate the loss of functionality of hospitals due to physical damage (structural and non-structural) is proposed. The functionality loss is determined by coupling detailed building damage assessments with the performance levels and the functionality classes defined by Yavari *et al.* (2010). The methodology is extended to consider functionality loss of service areas (i.e., ERs, ICU, Labs, etc.) on each floor independently. The functionality of each service area of the hospital is quantified assuming that the Functionality Classes (Fully Functional, Functional, Affected Functionality, and Not Functional), defined in Table 2.1, represent 0, 25, 50, 100% loss of functionality, following a similar rationale to that presented by Yi *et al.* (2019). For example, if a service area is in the Affected Functionality Class, the ability of hospital staff to provide their baseline level of care is reduced by 50%. To limit the

scope of this study, it is assumed that the hospital lifelines (i.e., water, power, and gas supply) will not be interrupted and will rely on the backup systems for continuity. Likewise, staffing (i.e., physicians, nurses) is assumed to be unaffected by the earthquake.

The Functionality Class, $FC_j$, of a service located in floor $j$ is determined using a decision tree diagram developed by Yavari *et al.* (2010) that accounts for all possible combinations of Performance Levels, for structural and nonstructural systems, denoted by $PL_{Str}$ and $PL_{NStr}$, respectively. The performance level of the systems (ranging from Performance Level 1 for no damage to Performance Level 4 for extensive damage), is determined by fault tree analysis. Performance levels are associated with the damage states of the relevant hospital building components. The proposed relationships are developed by mapping the damage state description from the FEMA P-58 fragilities to the corresponding performance level description provided by Yavari *et al.* (2010). From the damage output, the most likely Damage State, $DS$, is used to determine the corresponding Performance Level, $PL_i$, for each component, $i$. Then, the Performance Levels, $PL_{Str}$ and $PL_{NStr}$, for structural and non-structural systems, respectively, are taken as the most unfavorable Performance Level of each of the components considered. The approach used to map is summarized in Figure 3.3, and is also represented in the following equations:

$$FC_j = f(PL_{Str}, PL_{NStr}) \quad (3.19)$$

$$PL_{Str} \text{ or } PL_{NStr} = \max(PL_i) \quad (3.20)$$

$$PL_i = \text{mode}(DS) \quad (3.21)$$

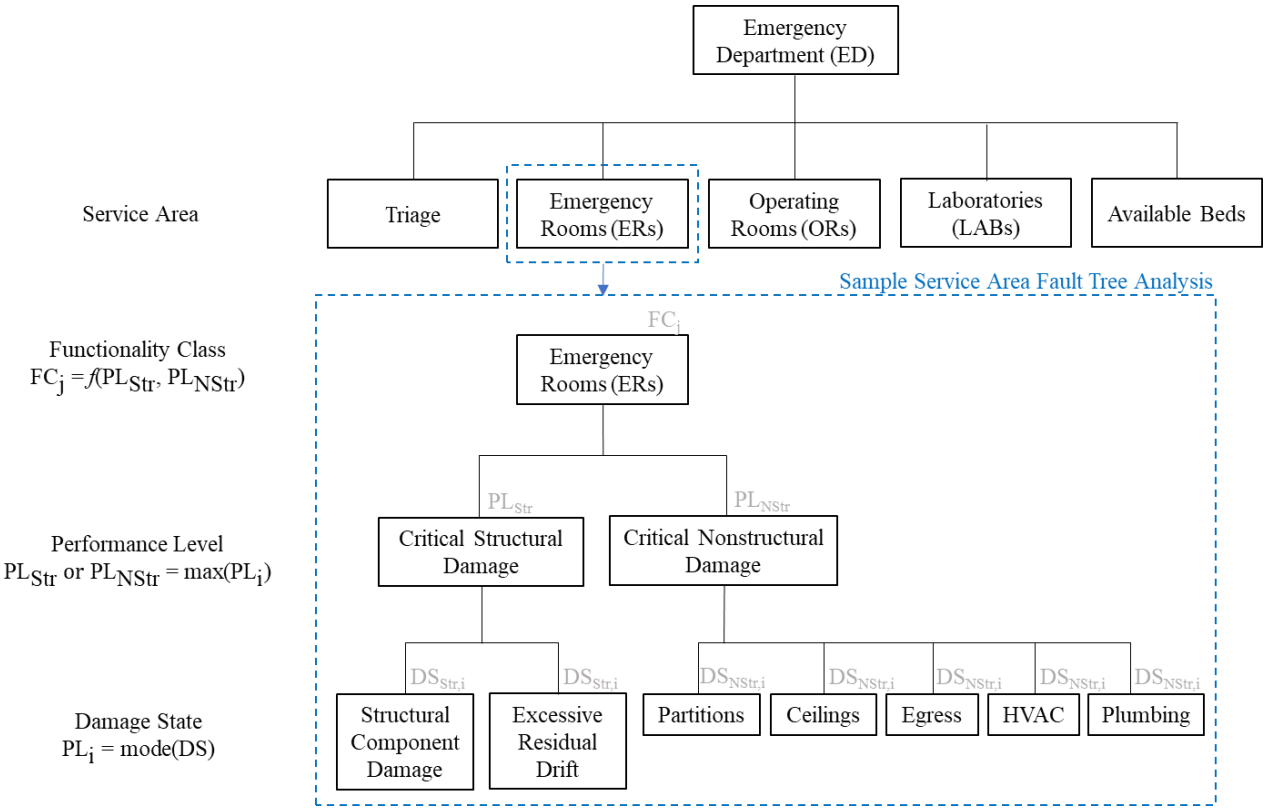


**Figure 3.3 Functionality loss assessment approach incorporating the fault tree analysis method.**

For each $k_C$ Monte Carlo simulation, the functionality loss of the service areas on each floor is estimated and the median functionality loss output that characterizes the post-earthquake ED capacity is determined. Determining the median value of the post-earthquake ED capacity is not trivial because functionality losses of services areas may affect the overall ED capacity to varying degrees. This problem can be addressed by leveraging the DES model that is described in the next section. Further details of the approach to identify the median post-earthquake ED capacity are presented later in the case study.

## 3.5 Discrete event simulation model

Discrete Event Simulation (DES) is used to provide rapid estimates of the ED surge capacity after an earthquake scenario. ED capacity is defined as the number of injured patients that can be

effectively treated without exceeding unacceptable (i.e., life-threatening) patient waiting times (Yi *et al.*, 2010). Hospital ED capacity is expressed in terms of the critical arrival rate at which patients could no longer be accepted. Surge capacity is the increased or decreased capacity available in the aftermath of disasters such as earthquakes (Gregory R., 2016). Hospital capacities can swell with an influx in staff or beds, or shrink if areas of the hospital are not usable due to loss of function.

Once the baseline DES model representing the steady-state condition is calibrated, the results from the functionality loss assessment are utilized to update the ED services areas' capabilities. To represent the increase in healthcare demand due to patients from the surrounding area in the disaster condition, the surge calculated from Phase 2 is added to the steady-state patient arrival. The DES model is thus able to simulate the emergency response of the ED. The model simulates patient flow through the different stages within the ED based on the severity of injuries and provides relevant information such as wait times (WT) for different services, and overall patient length of stay (LOS). The proposed DES model is simple, generic, and versatile, so it can be easily adapted to represent any ED. The model consists of a set of probability distributions governing the flow of patients through different stages within the ED according to the severity level of injury. The structure of the model conforms to the conceptual input-throughput-output framework of ED operations proposed by Yi *et al.* (2010) reflecting all essential care processes (stages) that substantially contribute to ED overcrowding. Figure 3.4 shows the patient routing in the following order: Triage, Emergency Room (ER), Laboratory, Operating Room (OR), Recovery Room (RR), or Post Anesthesia Care Unit (PACU) followed by Admission (Inpatient Bed) or Discharge. The model is implemented in JaamSim, an open-source simulation software package that includes a graphical user interface, and a full set of built-in objects for DES model building (King and Harrison, 2013).

Patient arrivals are simulated with a non-stationary Poisson process (Gross *et al.*, 2008), in which an exponential distribution governs the time between arrivals. The mean patient arrival rate is assumed to be constant and is calculated based on annual ED visits. After the earthquake, it is assumed that the steady-state patient arrival is constant, while the earthquake injured patients arrive within two to four days as determined from the surge estimation obtained from Phase 2. The DES model does not account for the effect of overcrowding on the efficiency of ED operations. Furthermore, to simplify the multitude of patient routings as a function of the specific type of injury (e.g., trauma, cardiology), the model classifies patients as a function of their acuity i.e., green, yellow or red codes, as seen in Figure 3.4. Patients follow a route based on the severity of their injuries; hence, patients with the same color code are assumed to have the same routing and consequently similar length of stay.

Upon arrival, patients are triaged by a specialized nurse or physician who determines the urgency by assigning three different color codes for patients: green, yellow, and red. Patients arriving under normal circumstances (steady-state) are assigned a color code using a discrete probability distribution, which is an adjustable parameter in the model. Earthquake-injured patients are assigned a severity level as determined via multi-severity casualty estimation, which is then matched to a corresponding color code as described earlier. In the simulation, hospital staff attends to patients on a first-come-first-served basis. Each patient's WT is tracked, and exceedances of permissible WTs in all ED stages are recorded.

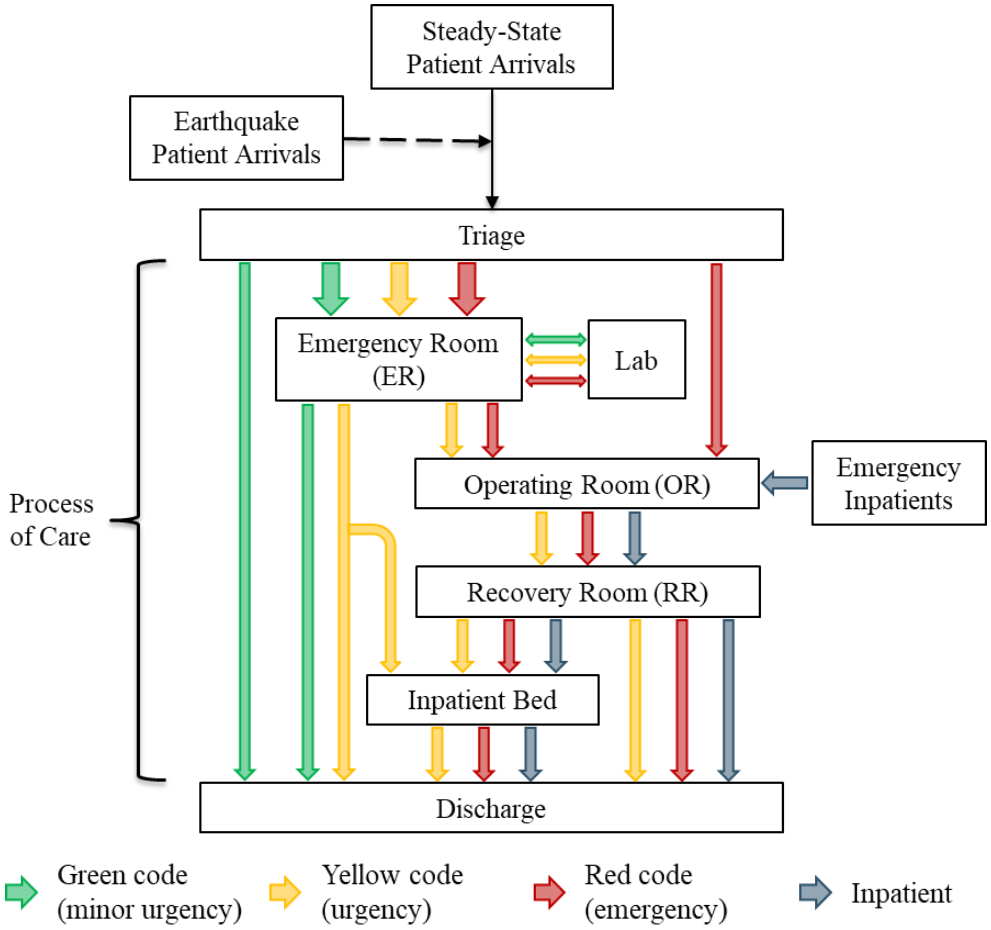


**Figure 3.4 Patients flow within the Emergency Department (modified after Yi *et al.*, 2010).**

After triage, an ED-specific discrete probability distribution is used to determine whether the patient is sent to ER, OR, or is discharged. Most patients are sent to ERs, where a physician examines the patient and orders laboratory tests (e.g., X-rays, CT scans) if necessary. After receiving treatment at an ER, the patient is either sent to an OR, an inpatient bed, or is discharged. Patients sent to the laboratory for additional examination will return to the ER to receive their final treatment once the test results are ready. High severity level patients that require surgery due to life-threatening injuries are sent directly from triage to ORs. After the OR, the patient is sent to a recovery room. Then, the patient will be admitted or discharged depending on the acuity of their condition. A separate decision probability for each color code in the simulation is used so that

patients with more acute conditions have, for example, a higher probability of being admitted to the hospital.

Each stage shown in Figure 3.4 has a defined capacity and service time. The capacity is determined by the physical space (e.g., number of rooms or beds) and by resource availability (e.g., nurses or physicians). If there are no rooms or medical staff available to treat a patient, the patient remains in the waiting room and the WT parameter increases. Service times, as well as all decision probabilities, are adjustable parameters in the model that are set based on data collected from hospital staff and on medical staff experience and judgment.

To improve the reliability of the DES model, data of the processes and operations within the ED is used to establish a baseline condition (Gul and Guneri, 2015b). A series of questions developed by Mitrani-Reiser *et al.* (2012) to capture ED baseline data (e.g., number of annual visits, WTs, service times) during normal conditions was adapted for use in this study. The data collected include information from hospital/ED information management systems, on-site observations, surveys, charts, interviews with the relevant staff, or time/motion studies. Validation can then be performed by comparing critical ED performance measures obtained from the model to actual data (Paul and Lin, 2012). For instance, this can be achieved by comparing the mean patient LOS and WT obtained from the model to the collected data for different patient types. Once validated in its steady state, the DES model can be used to investigate the ED post-earthquake surge capacity by evaluating various performance metrics. The model can not only be used to accurately capture the ED patient flow dynamics and identify improvement strategies for emergency response but also to provide a quantitative assessment of improvement measures before implementation.

# Chapter 4: Case Study

Vancouver General Hospital (VGH) is a major Level 1 trauma center, where the most severely ill patients in the City of Vancouver and surrounding areas are treated. VGH regularly receives patient transfers from throughout Western Canada and would be expected to play a major role in any disaster response in Metro Vancouver. The VGH emergency department (ED) has approximately 95,750 patient visits per year. In this case study, the methodology developed was implemented to investigate the surge capacity of this single ED following a hypothetical $M_w$9.0 CSZ scenario earthquake.

## 4.1 $M_w$9.0 Cascadia Subduction Zone earthquake scenario

In this case study, the Cascadia Subduction Zone (CSZ) megathrust fault, which has the potential to generate large-magnitude earthquakes in Southwest British Columbia, was considered. A suite of 30 physics-based simulations of an $M_w$9.0 earthquake scenario produced by Frankel *et al.* (2018) was utilized for the Case Study. The NBCC 2015 (NRCC, 2015) probabilistic estimates of the hazard compared to the mean response spectra of the suite of the 30 simulated ground motions at the VGH site, which is located approximately 120 km from the Cascadia Subduction Zone, are shown in Figure 4.1. For the period range of interest of the exposure model (i.e., 0.3 s to 1.0 s), the mean of the $M_w$9.0 simulations roughly aligns with the 475-year (i.e., 10% in 50 years) intensity level earthquake. This intensity level corresponds to a functional-level earthquake, which is often used to conduct function loss assessment and other resilience-based evaluations. It should be noted that the $M_w$9.0 mean spectrum exceeds the 975-year intensity level beyond the 1.0 s period due to basin amplification effects (Kakoty *et al.*, 2021). Basin amplification effects in the region are critical for tall buildings as discussed by Monfared *et al.* (2021). However, since the predominant

taxonomy in the hospital catchment area corresponds to low-rise wood structures (See Figure 4.3), these effects were not considered in this study. Furthermore, since the exposure is dominated by 0.3-second period structures (with demands even lower than that of the functional-level earthquake), few buildings will experience severe damage or collapse, and consequently, the number of red-code injuries might be limited.

For each earthquake scenario considered, bidirectional ground motion time histories were used to estimate the capacity, and the corresponding geomean response spectrum was used to estimate the demand. Three ground shaking intensity measures expressed in terms of spectral acceleration (SA) at building periods (T) of 0.3, 0.6, and 1.0 s, encompass the fragility data available for the building taxonomies in the exposure model of the catchment area generated by Natural Resources Canada (personal communication, 2018). These intensity measures were selected to capture the range of responses of the predominant building taxonomies in the inventory based on their fundamental period of vibration.

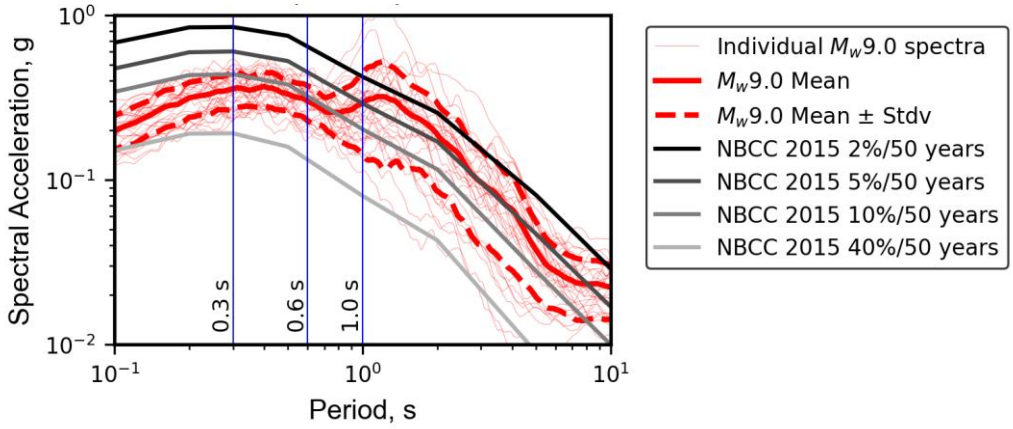


**Figure 4.1 Average response spectra of simulated Mw9.0 CSZ earthquake ground motions, and NBCC 2015 probabilistic estimates of the hazard with 2%, 5%, 10%, and 40% probability of exceedance in 50 years at the hospital site (VGH).**

## 4.2 Regional multi-severity casualty estimation

A regional multi-severity casualty estimation due to building damage for the 30 Mw9.0 earthquake scenarios was performed. It was assumed that injured people will travel to the closest hospital ED. Figure 4.2 (a) shows a map of the proximity to a health care facility as a function of driving distance for the City of Vancouver and surrounding areas (Statistics Canada, 2020), where the places closest to a hospital are shown in green, and the furthest, in red up to a maximum of 3 km. The estimated catchment area of VGH ED within Metro Vancouver is also highlighted in the plot. The exposure model of the estimated catchment area contains building taxonomies for 21,920 buildings. Figure 4.3 shows the breakdown of building typologies in the catchment area, which consist of mainly low-rise wood construction. The demographic distribution was also characterized at the building level, yielding a total resident population of 210,000.

For each of the 30 scenarios considered, 1,000 Monte Carlos realizations were performed to generate a distribution of patient arrivals, and the median realization was selected to characterize the surge in demand. Figure 4.2 (b) shows the median number of injuries per color code within the catchment area for the daytime earthquake occurrence. The factors driving the low number of serious injuries (i.e., red codes) are (1) the low spectral accelerations at the dominant period in the catchment area, and (2) the predominance of light-frame wood structures, which are less likely to cause red code injuries. Significant variability in the number of casualties for the different scenarios (e.g., Scenario 4 vs Scenario 29) can be observed. Likewise, the variation in the spatial distribution of the population over time (day, transit, and night) is also captured in the model. For instance, the median number of injuries was estimated at 174 (149 green codes, 25 yellow codes, and 0 red codes) for a nighttime earthquake Scenario 16. The time of earthquake occurrence results in a far lower number of casualties than if the event had occurred during the day due to the

predominance of commercial and office buildings in the area surrounding the hospital. For the daytime case (also Scenario 16), the median number of injuries was estimated at 382 (297 green codes, 85 yellow codes, and 1 red code). During transit, the median number of injuries was estimated at 269 (217 green codes, 52 yellow codes, and 0 red codes). In this case study, it was assumed that the earthquake-induced patients arrive at the ED within three days of the earthquake following a non-stationary exponential distribution, with 70% of injuries arriving the first day, 20% arriving the second day, and the remaining 10% arriving the third day.

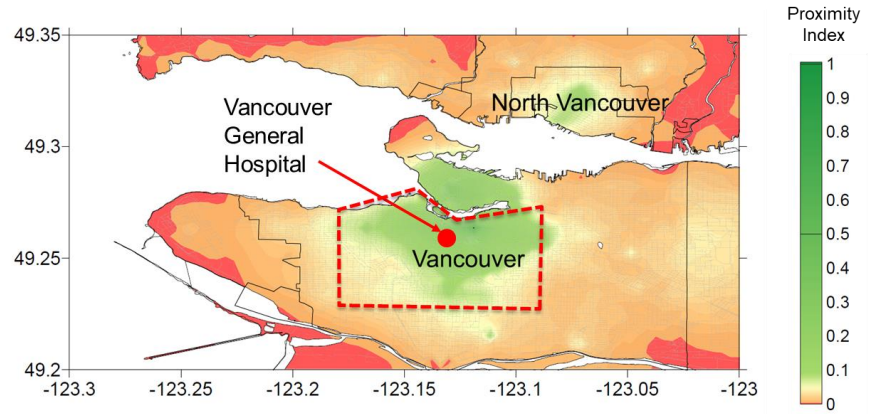


(a)

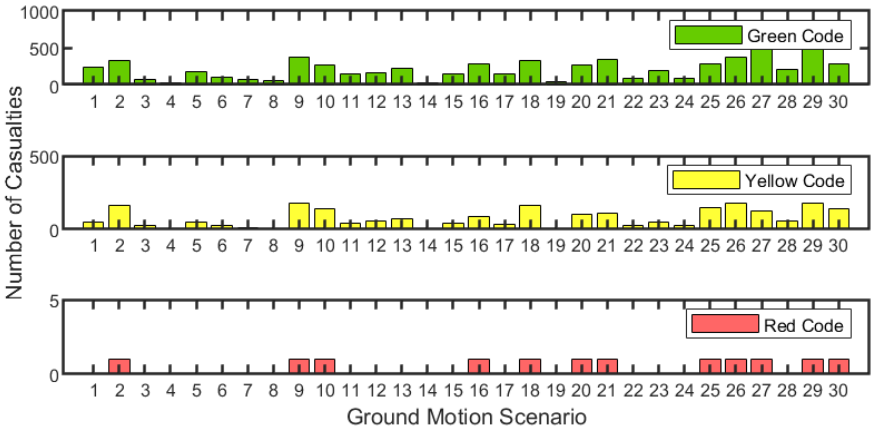


(b)

**Figure 4.2 (a) Proximity to health care and communities serviced by Vancouver General Hospital (data from Statistics Canada, 2020), and (b) the median daytime casualty estimates for the suite of 30 $M_w$9.0 CSZ earthquake scenarios.**

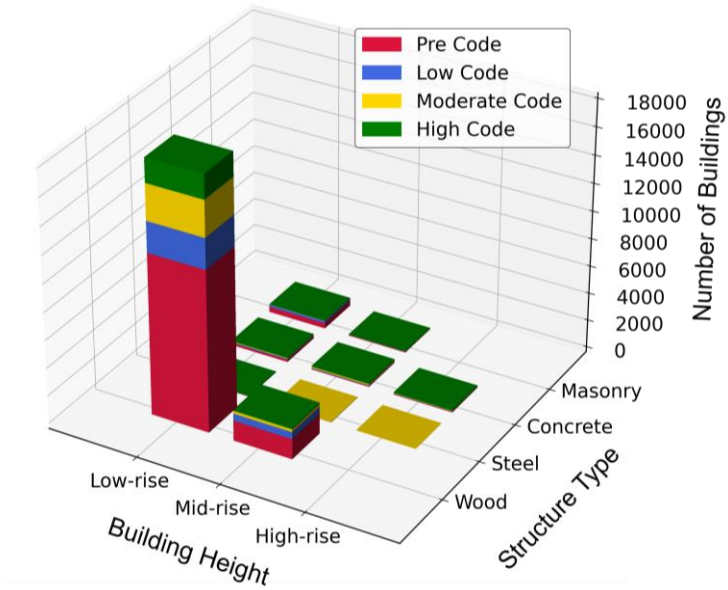


**Figure 4.3 General breakdown of building typologies on VGH catchment area (data from NRCan, 2018).**

## 4.3 Simplified non-linear structural analysis model

Jim Pattison Pavilion North (JPP North) houses the emergency response and critical care departments of Vancouver General Hospital (VGH) including the Emergency Department (ED), the Intensive Care Unit (ICU), Perioperative Services, and the helicopter landing facilities. The structural response of JPP North was estimated for a suite of 30 $M_w$9.0 ground motion scenarios. JPP North is a 4-story building built in 1978, with typical plan dimensions of 85.1 m x 76.8 m and a floor-to-floor height of 5.95 m. The structure has interstitial floors between each level above grade. These suspended floors do not contribute to the stiffness of the lateral force-resisting system, but the mass is lumped to the corresponding level. In the E-W direction, the lateral resisting system is an RC moment frame with typical 900 x 900 mm columns and 600 x 900 mm beams. In the N-S direction, the lateral system is an RC shear wall system with 250 mm and 400 mm thick walls, with longer walls located on the East side of the building. This discrepancy in the length of the walls on either side of the building is expected to cause an eccentricity of loading, which was

not accounted for in the simplified model. The concrete was modeled with a specified compressive strength of 28 MPa (~4 ksi) and the rebar with a nominal yield stress of 414 MPa (~60 ksi). The self-weight of the structure and superimposed dead loads were approximated as a uniform load of 8.75 kPa (183 psf) at all levels. Likewise, uniformly distributed live loads of 6.0 kPa (125 psf) were assumed at all levels. The calculated seismic weight is 84,500 kN for the typical floor (100% of dead load plus 50% of live load), and the assumed damping ratio is 2.5%.

NMFS models for each primary direction of the structure were constructed using OpenSeesPy. Data from a preliminary seismic assessment of the building (Bush Bohlman and Partners, personal communication, 2020), including structural drawings and a detailed structural analysis model, were used to develop and calibrate the NMFS model. From a detailed model, the reported fundamental periods in each orthogonal direction were 0.671s and 0.160s in the E-W (moment frame) and N-S (shear wall) directions, respectively. The flexural and shear stiffnesses were calculated following the procedure outlined in Xiong *et al.* (2016). After calibration of the elastic parameters, a modal analysis of the NMFS model was performed, and the resulting periods of vibration were 0.670s and 0.159s, respectively. Next, the tri-linear moment and shear response curves were estimated. The shear yield strength was derived from the base shear coefficient calculated using the National Building Code 1977 (NRCC, 1977), and the yield overstrength factor was assumed consistent with that reported in Table 5.5 of HAZUS (FEMA, 2020). The yield moment was determined using equations provided by Kuang and Huang (2011) that relate the yield moment and the yield shear force using a flexural-shear stiffness ratio, $\alpha_0$, of 3.67. The peak strengths were derived using the peak overstrength factor obtained from NBCC 2015 (NRCC, 2015), and the stiffness reduction factor was determined according to Provision 6.6.3.1.1 of ACI 318 (2014). Finally, the ultimate inter-story drift ratio at the complete damage state as per Table

6.4 of HAZUS (FEMA, 2020) was used to determine the ultimate strength points. The hysteretic material was defined with the pinching factors for strain (*pinchX*=0.40) and stress (*pinchY*=0.70), based on the findings of the calibration study with the refined model described earlier (refer back to Figure 3.2).

EDPs in both building directions for each of the 30 ground motion scenarios, as obtained from nonlinear response history analysis, are shown in Figure 4.4. The mean peak story drift ratios are 0.3% and 0.1% for the E-W and N-S directions respectively, well below the NBCC 2015 code limit of 2.5% under the 2475-year intensity level (NRCC, 2015). As expected, the story drift ratios are small because the suite of $M_w$9.0 motions is representative of a 475-year intensity level (i.e., functional-level) earthquake at the hospital location (see Figure 4.1). The peak floor accelerations range from 0.4 g to 0.6 g at the roof. The threshold floor acceleration at which extensive nonstructural damage is expected is 0.8 g (FEMA, 2020), and as such, it is expected that floor accelerations will govern the damage analysis.

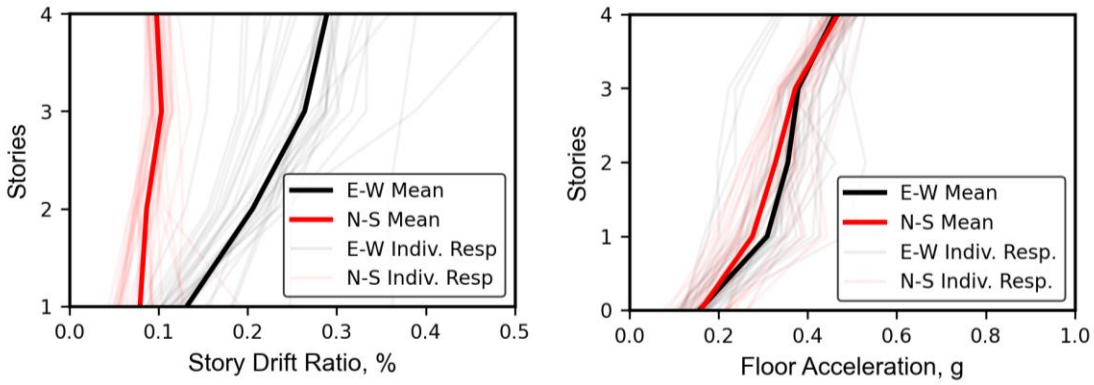


(a) (b)

**Figure 4.4 Seismic response of the VGH ED building using an NMFS model for a suite of 30 Mw9.0 CSZ earthquake scenarios: (a) story drift ratios and (b) floor accelerations in E-W (RC moment frame) and N-S (RC shear wall) directions.**

## 4.4 Building performance assessment

A building performance model of the ED building was created for the both E-W (moment frame) and N-S (shear wall) directions of the building. Non-structural component quantities were obtained using the FEMA P-58 Normative Quantity Estimation Tool (FEMA, 2018) and adjusted according to available data (e.g., layout plans, mechanical, electrical, and medical equipment inventory). Component quantities were assumed to be constant in all stories based on available architectural drawings. Table 4.1 presents a comprehensive summary of the components, including quantities and their distribution throughout the building, and relevant fragility functions from FEMA P-58. If the construction details of the component were not available, it was assumed that the component was constructed in accordance with the building year of construction. For example, for this hospital building constructed in 1978, ceiling components (e.g., suspended ceilings or piping) were assumed to be unbraced as the seismic restrain requirements became more strict after 1995 in Canada (Assi and McClure, 2015).

The building performance model was used to conduct a damage assessment using the FEMA P-58 methodology. The EDPs obtained from the nonlinear time-history analysis for both orthogonal directions of the ED building were used as input to the analyses. For each of the 30 earthquake scenarios, 1,000 Monte Carlo realizations of the damage assessment were performed using Pelicun (Zsarnoczay and Kourehpaz, 2021).

**Table 4.1 Structural and non-structural components per story of the VGH emergency department.**

| ID | Component Description | Quantity | Unit | Location | EDP |
|---|---|---|---|---|---|
| B1041.002b | Moment Frame | 49 | 1 ea | 1 – 4 | Story Drift |
| B1044.092 | Shear Wall | 6053 | 144 sf | Grond level | Story Drift |
| B2022.001 | Curtain wall | 7760 | 30 sf | 1-4 | Story Drift |
| C1011.001a | Partition wall | 5980 | 100 lf | 1-4 | Story Drift |
| C3011.001a | Partition wall - finishes | 704 | 100 lf | 1-4 | Story Drift |

| | | | | | |
|---|---|---|---|---|---|
| C3032.003a | Suspended ceiling | 70350 | 250 sf | 1-4 | Acceleration |
| C3034.002 | Ceiling - independent pendant lighting | 1057 | 1 ea | 1-4 | Acceleration |
| D2021.011a | Plumbing - cold or hot potable | 7000 | 1000 lf | 1-4 | Acceleration |
| D4011.021a | Plumbing - fire sprinkler water piping | 15477 | 1000 lf | 1-4 | Acceleration |
| D4011.031a | Plumbing - fire sprinkler drop | 845 | 100 ea | 1-4 | Acceleration |
| D1014.011 | Elevator | 3 | 1 ea | Grond level | Acceleration |
| C2011.021b | Stairs | 3 | 1 ea | 1-4 | Story Drift |
| D3041.012a | HVAC ducting (sectional area>6 sq.ft) | 1940 | 1000 lf | 1-4 | Acceleration |
| D3041.011a | HVAC ducting (sectional area<6 sq.ft) | 4157 | 1000 lf | 1-4 | Acceleration |
| D3041.031a | HVAC drops / diffusers | 1106 | 10 ea | 1-4 | Acceleration |
| D3041.041a | HVAC - variable air volume box | 554 | 100 ea | 1-4 | Acceleration |

## 4.5 Functionality loss assessment

The post-earthquake functionality of the ED service areas per floor was determined for each Monte Carlo realization of the damage assessment. The most likely Damage State of each component was linked to a Performance Level, ranging from 1 to 4. Table 4.2 shows a list of the Performance Levels associated with each Damage State of the hospital building components considered in the study. Once the Performance Level of the structural and non-structural systems was determined, the Functionality Class of each floor was assigned using the decision tree diagram developed by Yavari *et al.* (2010). The ability to treat patients is then taken as the percent functionality assigned via Functionality Classes (0, 50, 75, 100% corresponding to Not Functional, Affected Functionality, Functional, and Fully Functional class, respectively) for the corresponding service areas on each floor (see Table 4.3). For instance, if the third story is determined to be in the "Affected Functionality" class for one of the realizations, both the OR and PACU capacities are reduced by half, representing a 50% functionality loss.

**Table 4.2 Performance Level and associated Damage State of hospital building components.**

| ID | Component Description | Performance Level (1-4) | | | | |
|---|---|---|---|---|---|---|
| | | No Dmg. | DS1 | DS2 | DS3 | DS4 |
| B1041.002b | Moment Frame | 1 | 1 | 2 | 3 | 4 |
| B1044.092 | Shear Wall | 1 | 2 | 3 | 4 | - |
| - | Residual Drift[1] | 1 | 2 | 3 | 4 | - |
| B2022.001 | Curtain wall | 1 | 1 | 2 | - | - |
| C1011.001a | Partition wall | 1 | 2 | 3 | 4 | - |
| C3011.001a | Partition wall - finishes | 1 | 2 | - | - | - |
| C3032.003a | Suspended Ceiling | 1 | 2 | 3 | 4 | - |
| C3034.002 | Ceiling - independent pendant lighting | 1 | 2 | - | - | - |
| D2021.011a | Plumbing -Cold or Hot Potable | 1 | 1 | 2 | - | - |
| D4011.021a | Plumbing - Fire Sprinkler Water Piping | 1 | 1 | 2 | - | - |
| D4011.031a | Plumbing - Fire Sprinkler Drop | 1 | 1 | 2 | - | - |
| D1014.011 | Elevator | 1 | 1 | 2 | 3 | 3 |
| C2011.021b | Stairs | 1 | 1 | 2 | 3 | - |
| D3041.012a | HVAC ducting (sectional area > 6 sq.ft) | 1 | 2 | 3 | - | - |
| D3041.011a | HVAC ducting (sectional area < 6 sq.ft) | 1 | 2 | 3 | - | - |
| D3041.031a | HVAC Drops / Diffusers | 1 | 2 | - | - | - |
| D3041.041a | HVAC - Variable Air Volume box | 1 | 2 | - | - | - |

[1] No residual drift (No Damage) is presented in Performance Level 1. Residual drift <0.7% (DS1) for Performance Level 2. Residual Drift <0.7%, 2.0%> (DS2) for Performance Level 3. Residual Drift >2.0% (DS3) for Performance Level 4.

The damage outcomes from the FEMA P-58 analysis for each of the 1,000 Monte Carlo simulations were used to develop a distribution of possible functionality loss outcomes. To determine the median post-earthquake ED capacity, which is directly related to the functionality of the services areas, the simulation model was leveraged to perform a sensitivity analysis of the impacts of all possible functionality outcomes on the overall ED capacity. The sensitivity analysis is performed by incrementing the arrival rate until the ED is overcrowded (i.e., WTs on ERs or ORs exceed their performance threshold). The results of these analyses are presented in Figure 4.5. It is observed that the overall ED capacity can be reduced from 15.0 pat./hours (baseline) to 11.5 pat./hour, representing an overall capacity loss of 23%.

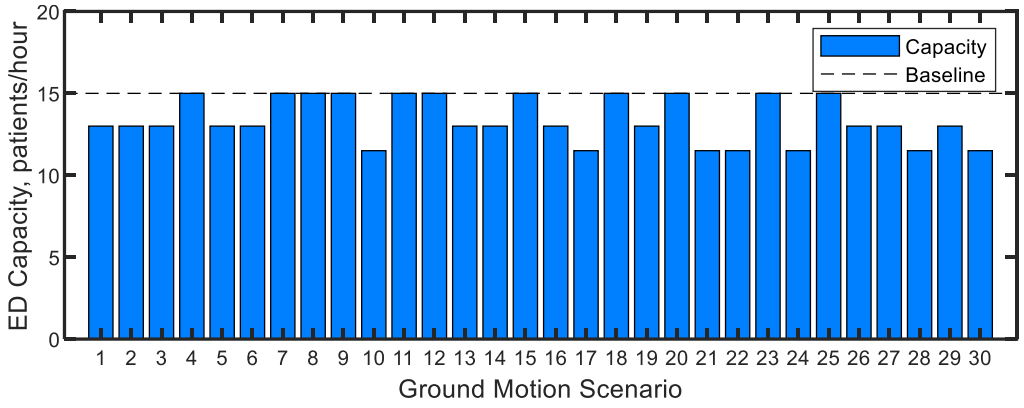


**Figure 4.5 Median ED capacity for the 30 Mw9.0 CSZ earthquake scenarios.**

## 4.6 Surge capacity modeling

To build the DES model, first, probability distributions governing the patient routing (presented in Figure 3.3) must be determined. Additional data is also required, including services times, and the capacities of each stage of patient care expressed in terms of the number of patients that can be treated at the same time (e.g., number of ORs). For this case study, ED-specific data were collected in consultation with Vancouver Coastal Health, through personal communication with the Decision Support – System Improvement team (Vancouver Coastal Health, personal communication, 2020). Table 4.3 presents the ED treatment areas per floor, and the main parameters used to set up the DES model. As per the health authority's regulations (e.g., CIHI, 2005), the maximum allowable WTs in ERs and ORs considered was two hours.

**Table 4.3 ED capacity and service time assumptions within the DES model.**

| Floor | ED Treatment Areas | Capacity[1] (# of units) | Service time[2] (min) | Distribution | Source |
|---|---|---|---|---|---|
| 1 | Triage | 4 | 15 | Poisson | Personal Communication |
| 1 | Emergency Room (ER) | 45 | 180 | Triangular | Personal Communication |
| 2 | Lab (Imaging/ X-ray) | 4 | 15 | Triangular | Personal Communication |
| 2 | Lab Turnaround | 4 | 40 | Triangular | Hawkins (2007) |
| 3 | OR - Utilization | 23 | 197 | Triangular | Personal Communication |

| | | | | | |
|---|---|---|---|---|---|
| 3 | OR - Turnover | 23 | 36 | Triangular | Mazzei (1994) |
| 3 | Recovery Rooms (RR) | 23 | 192 | Triangular | Personal Communication |
| 4 | In-patient Beds | 450 | 4896 | Triangular | Personal Communication |

[1] Determined by the physical space (e.g., # of rooms) and resource availability (e.g., # of triage nurses).
[2] Mean time to treat one patient.

The total annual number of visits to the VGH ED is 95,750. The derived steady-state patient arrival rate, during normal conditions, is 11 patients/min. From communications with the hospital staff, the percent of patients triaged under normal conditions that are green, yellow, and red code patients are 36%, 46%, and 18%, respectively. Annually, an average of 60% of the red code patients and 20% of the yellow code patients are sent to ORs, i.e., 20% of the total ED visits are sent to the OR. An annual average of 15% of out-patients is directly discharged after triage, while 21% of the patients are admitted to the hospital. The daily normal patient arrivals and the additional earthquake patient arrivals for a representative scenario, as determined from the regional multi-severity casualty estimation, are summarized in Table 4.4.

**Table 4.4 Patient demand at the ED during earthquake emergency response.**

| Patient Acuity | Daily Steady-State Patients | Additional Earthquake Patients[1] |
|---|---|---|
| Green Codes (Minor Urgency) | 94 (36%) | 277 (73%) |
| Yellow Codes (Urgency) | 120 (46%) | 104 (27%) |
| Red Codes (Emergency) | 93 (18%) | 1 (1%) |

[1] Median patient distribution of one representative scenario (daytime).

### 4.6.1 Validation of the DES model

Once the DES model was populated with the actual ED data, it was calibrated under normal operating conditions. The LOS by patient category, time to physician initial assessment, WTs in ERs and ORs, and average occupancies were used to validate the DES model. The baseline simulation results were calibrated to within 0~1% of the hospital data, as shown in Table 4.5.

**Table 4.5 Validation of the Baseline Model during normal operating conditions.**

| Variable (Average Times) | Simulation | Collected Data | Error |
|---|---|---|---|
| Triage Wait Time | 9.03 min | 9.00 min | 0.3% |
| Physician Initial Assessment Time | 94.66 min | 95.00 min | 0.4% |
| ER utilization time | 301.82 min | 302.00 min | 0.1% |
| OR Utilization Time | 59.96 min | 60.00 min | 0.1% |
| Length of Stay | 6.55 h | 6.52 h | 0.5% |
| Length of Stay (green-tagged patient) | 4.45 h | 4.43 h | 0.5% |
| Length of Stay (yellow-tagged patient) | 7.46 h | 7.37 h | 1.2% |
| Length of Stay (red-tagged patient) | 8.43 h | 8.48 h | 0.6% |
| Length of Stay (in-patients) | 6.96 d | 7.00 d | 0.6% |

For the calibration of the DES model, the parameters defined in Table 4.3 (i.e., service times, and capacity of the service areas), as well as the collected statistics (e.g., patient color code probability distribution at the arrival), were constants. The rest of the probability distributions governing the patient routing (as defined in Figure 3.4) were variables to be calibrated. For instance, based on the collected data, 60% of the red code patients are sent to ORs, but the probability of whether they are going directly after triage or after visiting the ERs is not given. After the calibration, it was defined that red codes have 0.25 probability to be directly sent to ORs after triage, while the rest are sent to an ER. From the ER, red codes have 0.47 probability to be sent to an OR, and 0.53 probability to be admitted after they finish their treatment in the ER. In other words, after the calibration, it was defined that 25% of the red code patients are sent to ORs after being triaged, and 35% of them are sent to ORs after being treated in an ER, respectively.

A sensitivity analysis of the validated model was performed to find the steady-state hospital ED capacity. From the sensitivity analysis, the maximum allowable rate of patient arrivals to ensure the maximum ER and OR WTs did not exceed the two hours limit was determined to be 15 patients/hour. The sensitivity analysis was also used to identify process bottlenecks. In this case

study, both the ERs and ORs were identified as having the largest impact on overall patient LOS. The graphical representation of the DES model in JaamSim software, as well as a detailed explanation of the sensitivity analysis to estimate capacity, is provided in Appendix B.

### 4.6.2 Simulation in a disaster earthquake condition

The simulation of the ED required an initial warm-up period to reach a steady state. Once the steady-state was reached, the ED performance was simulated for 30 days. The earthquake was induced two days following the warm-up period, triggering the loss of ED capacity and the arrival of earthquake-injured patients. The DES model was run for each of the 30 earthquake scenarios, using the patient arrival rate determined from the median multi-severity casualty estimates and the corresponding reductions in functionality for each service area associated with the median ED capacities as derived from the functionality loss assessment.

## 4.7 Results and discussion

The numerical outputs of the simulation are expressed as patient WT in each stage simulated in the ED and the total patient LOS. The WT is calculated as the idle time during which the patient is not assisted by any staff member until a spot in the corresponding ED stage (i.e., triage, ERs, ORs) is available. For example, ER room WT is the idle time before seeing a physician once registered and triaged. The mean LOS for each patient color code was computed every 12 hours and includes both admitted patients (time of arrival to the time of hospital admission) and discharged patients (time of arrival to the time of discharge). The LOS was calculated as the sum of the mean WT plus service times on each ED stage. The demand and capacity are presented in terms of patient arrivals. When the ratio of demand over capacity (DCR) reaches a critical value of 1.0, this indicates that the ED is operating at its maximum capacity, with any further increase resulting in excess WTs.

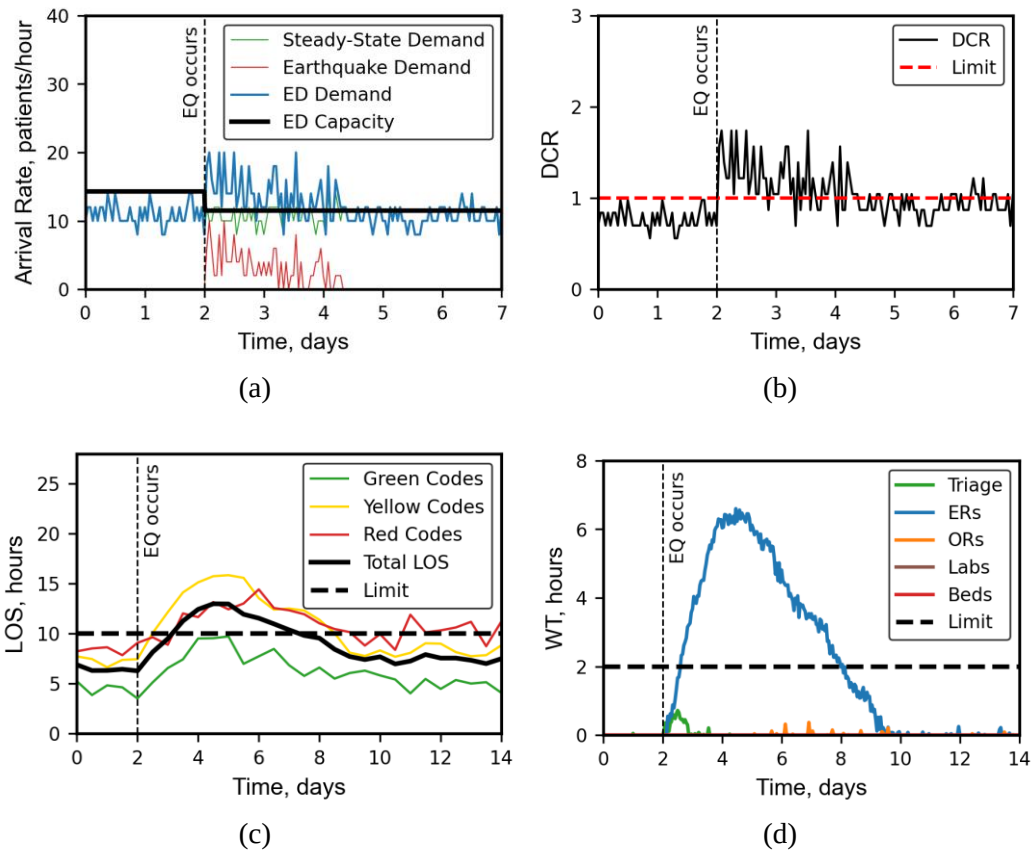


**Figure 4.6 Outputs of a single daytime earthquake scenario, including the temporal variation of (a) median demand and capacity arrival rates, (b) median demand-to-capacity ratio (DCR), (c) mean patient length of stay (LOS), (d) mean patient wait times (WT). Earthquake occurrence at time = 2 days.**

The simulation results for one earthquake scenario are presented in Figure 4.6. In the selected simulation, the healthcare demand doubled due to the earthquake patient arrivals, and the overall ED capacity was reduced by 23% immediately after the earthquake occurs, as shown in Figure 4.6 (a). This reduction in ED capacity is due to the physical damage on the first floor of the building and consequently, a loss of functionality of the ERs. In Figure 4.6 (d), it is can be seen that the ERs become the bottleneck of patient flow, with a maximum mean WT of approximately 6.5 hours. Yellow code patients receive most of their treatment in an ER and require more time and resources than green-code patients to be treated; this results in an average LOS in excess of

10 hours as shown in Figure 4.6 (c). The patient arrival rate returns to the pre-event rate on day four, at which point the DCR oscillates around 0.95, as shown in Figure 4.6 (b), which represents an increase in DCR from the pre-earthquake baseline value of 0.85 due to the loss of functionality in the building.

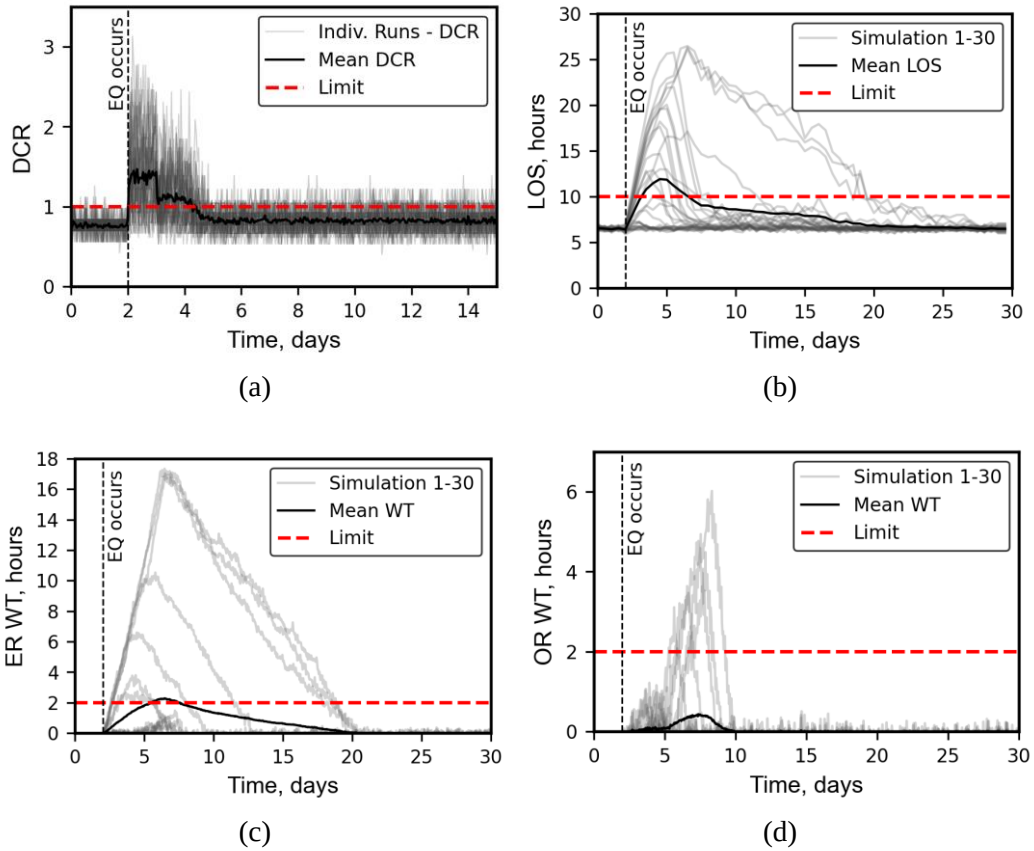


**Figure 4.7 Summary outputs of all 30 daytime earthquake scenarios, including the temporal variation of (a) mean demand-to-capacity ratio (DCR), (b) mean patient length of stay (LOS), (c) mean emergency room wait times (ER WT), and (d) mean operating room wait times (OR WT). Earthquake occurrence at time = 2 days.**

The ED response for all 30 $M_w$9.0 CSZ earthquake scenarios simulated is summarized in Figure 10. The demand to capacity ratio illustrated in Figure 4.7 (a) shows the increase of healthcare demand that occurs between day two and day five. During this time, the demand exceeds the capacity by up to three times in some scenarios. After day five, it is observed that the

mean DCR increases from the pre-event baseline of 0.85 up to 0.90. The observed increase in demand to capacity ratio is due to slight to moderate damage to the structural and non-structural components of the hospital building and, consequently, a slight loss of functionality after the earthquake. The patient arrival rate returns to the pre-earthquake rate after day five. However, the ED performance metrics continue to increase with maximum values observed after three or five days of the earthquake. As observed in Figure 4.7 (b) and (c), the mean patient LOS and ER WT peak at day 5 and 7, respectively. For the most critical of the $M_w$9.0 simulations, it is predicted that the ED will take up to 20 days for the LOS and ER WT to return to their baseline levels. The mean OR WT peaks at approximately day 7, as shown in Figure 4.7 (d), reflecting the accumulation of delays in the preceding stages of the DES model.

Both WT and LOS increase substantially from normal operating conditions to disaster conditions, with the ER WT reaching up to 17 hours and with the OR WT reaching up to 6 hours in the most unfavorable condition. The mean patient LOS increases up to four times from 6.5 to 26 hours. From these results, it can be concluded that, while the ED hospital building experiences minimal losses of functionality and performs well under the earthquake scenario analyzed, the increase in healthcare demand due to physical damage in the catchment area has a greater impact than the loss of functionality on the ED performance metrics. These observations apply to this case study only and are not generic because they reflect both the building stock and resulting demand as well as the performance of the hospital building investigated. Additionally, these results and findings are expected to vary for different earthquake intensity levels, indicating the need to analyze the ED performance for other plausible earthquake scenarios in the region.

The results presented in Figures 4.6 and 4.7 represent the daytime occurrence of the earthquake scenarios. ED performance metrics for three times of day of the earthquake occurrence:

day (2 pm), transit (5 pm), and night (2 am), were also calculated. The time of earthquake occurrence impacts the healthcare demand due to the variability in the population model throughout the day in the neighborhoods serviced by the ED. In this case study, the baseline patient arrival rates increase by a factor of 3.0, 2.0, and 1.5 for the daytime, transit, and nighttime earthquake occurrence, respectively. The analysis of the results shows that the maximum LOS times for the mean of the thirty simulations are 12, nine, and seven hours, for the day, transit, and night earthquake occurrences, respectively. For the emergency rooms (ERs), previously identified as the bottleneck in the patient flow, the target WT of two hours is exceeded on 7, 6, and 4 out of the 30 simulations for the day, transit, and night earthquake occurrences, respectively. Results show that maximum ER WTs for the mean of the thirty simulations are 2.2, 1.5, and 0.7 hours, respectively. The nighttime earthquake occurrence has a lesser impact on ED performance metrics because a high proportion of buildings in the surrounding area of the hospital are commercial and office buildings, many of the occupants in these buildings travel outside of the catchment area at night.

The implementation of different emergency plans in the hospital ED can also be analyzed using the proposed methodology. Mitigation measures may include adding resources (i.e., physicians, emergency rooms), ambulance diversion, or the deployment of field hospitals. In this case study, emergency rooms (ERs) were identified as the bottleneck. The results also revealed that both yellow and green code patients experienced longer WTs in ERs. Thus, a possible solution to relieve the ED overcrowding is the deployment of field hospitals with additional ERs. Since less severe patients need relatively few resources, the implementation of field hospitals with ERs for simple treatments that can be set up very quickly for green code patients was studied. This mitigation measure was also considered by Ceferino *et al.* (2020), but instead of installing

additional ERs, they evaluated the use of field hospitals with ORs to be used for patients with life-threatening injuries.

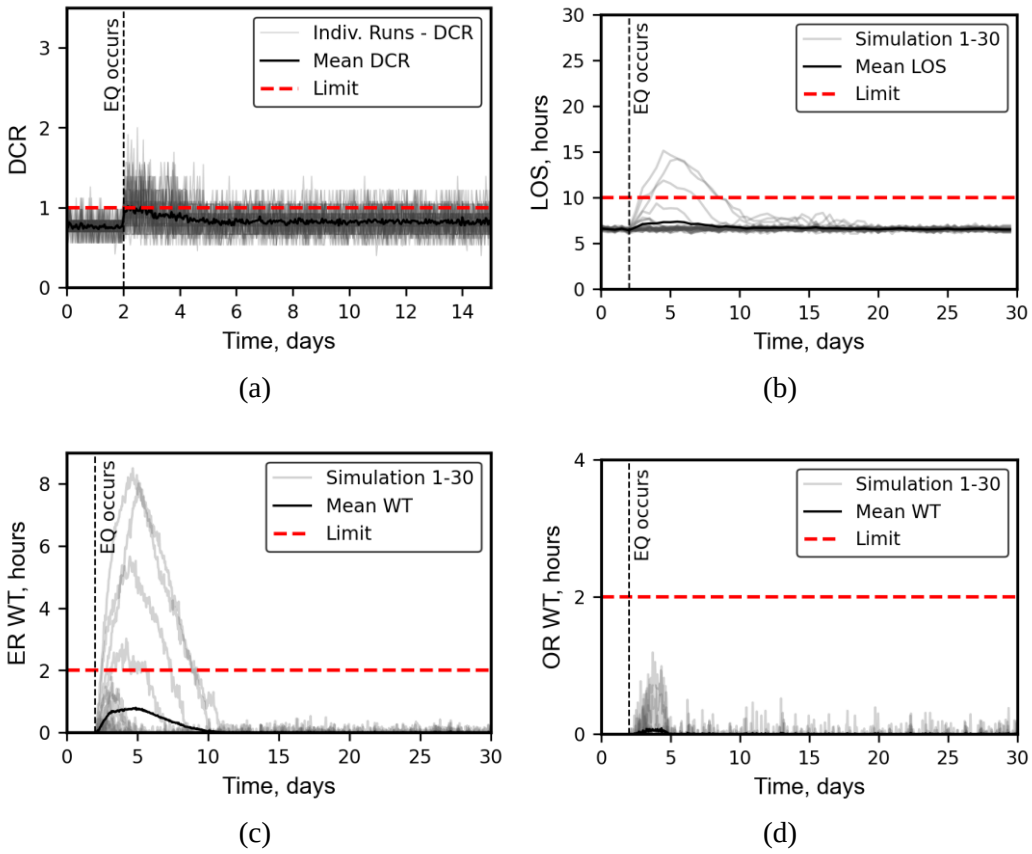


**Figure 4.8 Impacts of possible mitigation measures: (a) demand-to-capacity ratio (DCR), (b) mean patient length of stay (LOS), (c) emergency room wait times (ER WT), and (d) operating room wait times (OR WT). Earthquake occurrence at time = 2 days.**

To evaluate this emergency response plan of providing field hospitals to all green code patients, the DES model was analyzed assuming all green code patients were redirected away from the ED. As shown in Figure 4.8, the implementation of this plan reduces the healthcare demand by 33%. Consequently, the mean peak LOS is reduced from 12 to 7 hours, a 42% decrease from the original case study (see Figure 4.7). The average peak WT in the ERs decreases by 68%, from 2.2 to 0.7 hours. The mean OR WTs decreased to almost zero, reflecting the overcrowding relief

in the bottleneck stages of the DES model. This simple exercise serves to demonstrate the value of the proposed framework in evaluating the effectiveness of different mitigation measures or emergency response interventions.

# Chapter 5: Conclusions

## 5.1 Summary of findings

In this study, a framework is developed to investigate the post-earthquake functionality and surge capacity of hospital emergency departments (ED) using discrete event simulation (DES). A current research gap in the simulation of EDs was identified to be the lack of a model capable of accounting for the damage to a wide range of components that controls the post-earthquake functionality of relevant healthcare services within a hospital building. To address this gap, the methodology advances existing models by accounting for a wider range of building component damage, as well as their interdependencies, on the post-earthquake functionality loss assessment. The methodology explicitly links the structural response of a simplified nonlinear structural analysis model of a hospital building, and its expected earthquake damage, to the functionality loss of its services areas (i.e., emergency rooms, operating rooms, laboratories, etc.) on each floor. The use of simplified structural models facilitiates its adoption to assess the response of multiple EDs at a regional scale. Furthermore, the model captures the dynamics between demand and capacity of an ED during a disaster condition, providing relevant ED performance metrics such as wait time (WT) and length of stay (LOS) for patients with different injury severity levels. The methodology facilitates an improved understanding of the post-earthquake surge capacity and functionality of EDs. Moreover, the framework can be used to evaluate the effect of possible interventions within the ED, thus supporting the development of emergency response plans.

Thus, a current research gap in the simulation of EDs during an earthquake disaster is the implementation of a detailed functionality loss assessment that enables the evaluation of the micro-level behavior of EDs using performance metrics. The novelty of the proposed methodology lies

in: (1) accounting for the damage to a wide range of structural and non-structural components and the interdependencies between hospital systems in the functionality loss calculation; (2) incorporating simplified non-structural models capable of providing rapid estimates of the engineering demand parameters (EDPs) in each floor of the hospital buildings; making the method suitable to analyze multiple EDs in a regional scale; (3) capturing the inherent variability of the demand surge and capacity estimation by employing ground motion intensity maps, and consistent acceleration time histories in a scenario-based framework; and (4) enabling the evaluation of the ED performance through metrics such as wait times on relevant service areas, and the length of stay according to patients acuity.

The methodology was used to model a case study hospital ED in Vancouver, Canada subjected to 30 physics-based simulations of an $M_w$9.0 CSZ earthquake scenario. The case study hospital building experienced minimal structural and non-structural damage and little to no functionality loss in all the earthquake scenarios considered. The post-earthquake demand to capacity ratio (DCR) increased from a mean baseline of 0.85 up to 0.90, indicating the ED would be operating at almost its maximum capacity. The surge in demand after the earthquake, however, had a greater impact than the functionality loss on the ED performance, causing the mean LOS to nearly double from 6.5 to 12 hours with the peak LOS increasing up to four times to 26 hours. The mean ER room WT exceeded its limit of 2 hours, reaching up to 17 hours in the most unfavorable simulation. The DES model results were used to identify ERs as the bottleneck in the ED patient flow. The deployment of field hospitals to treat patients with the lowest injuries severity was evaluated as an emergency plan to mitigate ED overcrowding. This mitigation measure reduced the healthcare demand by 33%, in turn reducing the mean LOS and ER room WT by 42% and 68% below the original case study, respectively. It was demonstrated that the methodology can be

utilized as a decision support tool to improve healthcare disaster planning. While the case study focuses on a specific ED, the model proposed is generic and can be applied to any ED.

## 5.2 Limitations and future studies

The methodology serves as a good point of departure to study the post-earthquake performance of EDs. However, further advancements can be made. For instance, the simplified 2D nonlinear structural analysis model of the hospital building can be advanced to consider a three-dimensional analysis by coupling both horizontal directions. Furthermore, to improve the estimation of the earthquake-induced patient arrivals and their acuity, the model should also consider rescue and transport times. To improve performance metric calculations, prioritization of most urgent patients can be included in the DES model, in lieu of a 'first-come-first-serve' basis for treatment. In this study, the reduction of critical personnel and the interruption in services, such as water and electricity, were not considered. Future studies should consider the loss of critical lifelines and personnel, in addition to the physical damage, within the fault-tree analysis to estimate functionality loss. Another limitation of this study is examining a hospital ED as an isolated system. To advance this work, the complete network of EDs within a disaster region should be simulated. Furthermore, ED capacity estimates must be made in real-time so that they can be useful for disaster management.

## Bibliography

ACI Committee 318 (2014) *Building Code Requirements for Structural Concrete (ACI 318S-14) and Commentary (ACI 318SR-14)*.

Adams LM (2009) Exploring the Concept of Surge Capacity. *Online Journal of Issues in Nursing* 14(2). DOI: 10.3912/OJIN.Vol14No02PPT03.

Assi R and McClure G (2015) Evolution of the NBCC seismic provisions for operational and functional components in buildings. *Canadian Journal of Civil Engineering* 42(12): 993–999. DOI: 10.1139/cjce-2014-0219.

Benson M, Koenig KL and Schultz CH (1996) Disaster triage: START, then SAVE-a new method of dynamic triage for victims of a catastrophic earthquake. *Prehospital and Disaster Medicine* 11(2): 117.

Bentz EC and Collins MP (2001) Response-2000, Shell-2000, Triax-2000, Membrane-2000 User Manual. Available at: http://www.ecf.utoronto.ca/~bentz/r2k.htm.

Bruneau M and Reinhorn A (2007) Exploring the concept of seismic resilience for acute care facilities. *Earthquake Spectra* 23(1): 41–62. DOI: 10.1193/1.2431396.

Bruneau M, Chang SE, Eguchi RT, et al. (2003) A Framework to Quantitatively Assess and Enhance the Seismic Resilience of Communities. *Earthquake Spectra* 19(4): 733–752. DOI: 10.1193/1.1623497.

Ceferino L, Kiremidjian A and Deierlein G (2018a) Probabilistic Model for Regional Multiseverity Casualty Estimation due to Building Damage Following an Earthquake. *ASCE-ASME Journal of Risk and Uncertainty in Engineering Systems* 4(3). DOI: 10.1061/AJRUA6.0000972.

Ceferino L, Kiremidjian A and Deierlein G (2018b) Regional Multiseverity Casualty Estimation Due to Building Damage following a Mw 8.8 Earthquake Scenario in Lima, Peru. *Earthquake Spectra* 34(4). DOI: 10.1193/080617EQS154M.

Ceferino L, Mitrani-Reiser J, Kiremidjian A, et al. (2020) Effective plans for hospital system response to earthquake emergencies. *Nature Communications* 11(1): 1–12. DOI: 10.1038/s41467-020-18072-w.

Ceferino LA (2019) Effective Emergency Response Policies for Hospital Systems in the Wake of Time-varying Seismic Hazard. *Thesis Ph.D. Stanford University, California*. Available at: https://searchworks.stanford.edu/view/13250189.

CIHI (2005) Understanding Emergency Department Wait Times. *Canadian Institute for Health Information*. Available at: https://www-deslibris-ca.eu1.proxy.openathens.net/ID/210964.

Cimellaro GP, Fumo C, Reinhorn A, et al. (2009) Quantification of Disaster Resilience of Health Care Facilities. *Multidisciplinary Center for Earthquake Engineering Research Technical Report MCEER-09-0009*. Buffalo, New York.

Cimellaro GP, Reinhorn A and Bruneau M (2010) Seismic resilience of a hospital system. *Struct. and Infra. Eng.* 6(1): 127–144. DOI: 10.1080/15732470802663847.

Cimellaro GP, Reinhorn AM and Bruneau M (2011) Performance-based metamodel for healthcare facilities. *Earthquake Engineering & Structural Dynamics* 40(11): 1197–1217. DOI: 10.1002/eqe.1084.

Cimellaro GP, Ali Zamani Noori, Omar Kammouh, et al. (2016) Resilience of Critical Structures, Infrastructure, and Communities. *Pacific Earthquake Engineering Research Center PEER Report No. 2016/08*. Berkeley, California.

Derlet R, Richards J and Richard K (2001) Frequent Overcrowding in U.S. Emergency

Departments. *Academic Emergency Medicine* 8(2): 151–155. DOI: 10.1111/j.1553-2712.2001.tb01280.x.

Eberhard MO, Baldridge S, Marshall J, et al. (2010) The Mw 7.0 Haiti earthquake of January 12 , 2010 : USGS / EERI Advance Reconnaissance Team Report. *U.S. Geological Survey Open-File Report 2010–1048*. Reston, Virginia.

Eksir Monfared A, Molina Hutt C, Kakoty P, et al. (2021) Effects of the Georgia Sedimentary Basin on the Response of Modern Tall RC Shear-Wall Buildings to M9 Cascadia Subduction Zone Earthquakes. *Journal of Structural Engineering* 147(8). DOI: 10.1061/(ASCE)ST.1943-541X.0003067.

Fava G, Giovannelli T, Messedaglia M, et al. (2021) Effect of different patient peak arrivals on an emergency department via discrete event simulation: a case study. *Simulation*. DOI: 10.1177/00375497211038756.

Favier P, Rivera F, Poulos A, et al. (2017) Impact on Chilean Hospitals Following the 2015 Illapel Earthquake. In: *16th World Conference on Earthquake*, Santiago, Chile, 2017.

Favier P, Poulos A, Vásquez JA, et al. (2019) Seismic risk assessment of an emergency department of a Chilean hospital using a patient-oriented performance model. *Earthquake Spectra* 35(2): 489–512. DOI: 10.1193/103017EQS224M.

Fawcett W and Oliveira CS (2000) Casualty Treatment after Earthquake Disasters: Development of a Regional Simulation Model. *Disasters* 24(3): 271–287. DOI: 10.1111/1467-7717.00148.

FEMA (2003) FEMA 396: Incremental Seismic Rehabilitation of Hospital Buildings. *Federal Emergency Management Agency*. Washington D.C.

FEMA (2018) FEMA P-58-1: Seismic Performance Assessment of Buildings. Volume 1 – Methodology. *Federal Emergency Management Agency*. Washington D.C.

FEMA (2020) HAZUS Earthquake Model Technical Manual. *Federal Emergency Management Agency*. Washington D.C.

Frankel A, Wirth E, Marafi N, et al. (2018) Broadband Synthetic Seismograms for Magnitude 9 Earthquakes on the Cascadia Megathrust Based on 3D Simulations and Stochastic Synthetics, Part 1: Methodology and Overall Results. *Bulletin of the Seismological Society of America* 108(5A): 2347–2369. DOI: 10.1785/0120180034.

GEM (2021) The OpenQuake-engine User Manual. *Global Earthquake Model (GEM)*. DOI: 10.13117/GEM.OPENQUAKE.MAN.ENGINE.3.12.0.

Gross D, Shortle JF, Thompson JM, et al. (2008) *Fundamentals of Queueing Theory*. Fourth Edi. Hoboken, New Jersey.

Gul M and Guneri AF (2015a) A comprehensive review of emergency department simulation applications for normal and disaster conditions. *Computers & Industrial Engineering* 83(1): 327–344. DOI: 10.1016/j.cie.2015.02.018.

Gul M and Guneri AF (2015b) A discrete event simulation model of an emergency department network for earthquake conditions. In: *6th International Conference on Modeling, Simulation, and Applied Optimization (ICMSAO)*, Istanbul, Turkey, 2015.

Gul M, Guneri AF and Gunal MM (2020) Emergency department network under disaster conditions: The case of possible major Istanbul earthquake. *Journal of the Operational Research Society* 71(5): 733–747. DOI: 10.1080/01605682.2019.1582588.

Gunal MM (2012) A guide for building hospital simulation models. *Health Systems* 1(1): 17–25. DOI: 10.1057/hs.2012.8.

Hawkins RC (2007) Laboratory turnaround time. *The Clinical Biochemist* 28(4): 179–194.

Henderson AK, Lillibridge SR, Salinas C, et al. (1994) Disaster Medical Assistance Teams:

Providing Health Care to a Community Struck by Hurricane Iniki. *Annals of Emergency Medicine* 23(4): 726–730. DOI: 10.1016/S0196-0644(94)70306-X.

Jacques CC, Boston M and Mitrani-Reiser J (2014) Quantifying the performance of healthcare facilities in disasters: A multi-hazard approach. In: *10th U.S. National Conference on Earthquake Engineering: Frontiers of Earthquake Engineering*, Anchorage, Alaska, 2014.

Jacques CC, McIntosh J, Giovinazzi S, et al. (2014) Resilience of the Canterbury Hospital System to the 2011 Christchurch Earthquake. *Earthquake Spectra* 30(1): 533–554. DOI: 10.1193/032013EQS074M.

Joshi A and Rys M (2011) Study on the effect of different arrival patterns on an emergency department's capacity using discrete event simulation. *International Journal of Industrial Engineering* 18(1): 40–50.

Kakoty P, Dyaga SM and Molina Hutt C (2021) Impacts of simulated M9 Cascadia Subduction Zone earthquakes considering amplifications due to the Georgia sedimentary basin on reinforced concrete shear wall buildings. *Earthquake Engineering & Structural Dynamics* 50(1): 237–256. DOI: 10.1002/eqe.3361.

King DH and Harrison HS (2013) Open-source simulation software 'JaamSim'. In: *Winter Simulations Conference (WSC)*, Washington D.C., December 2013, pp. 2163–2171. DOI: 10.1109/WSC.2013.6721593.

Kuo KC, Banba M and Suzuki Y (2008) Loss Analysis Of Medical Functionality Due To Hospital's Earthquake-Induced Damages. In: *14th World Conference on Earthquake Engineering (14WCEE)*, Beijing, China, 2008.

Lanning F, Haro AG, Liu MK, et al. (2016) EERI Earthquake Reconnaissance Team Report: M7.8 Muisne, Ecuador Earthquake on April 16, 2016. *Earthquake Engineering Research Institute*.

Lin C-H, Kao C-Y and Huang C-Y (2015) Managing emergency department overcrowding via ambulance diversion: A discrete event simulation model. *Journal of the Formosan Medical Association* 114(1): 64–71. DOI: 10.1016/j.jfma.2012.09.007.

Lin Y-X, Lin Chi-Hao and Lin Chih-Hao (2021) A challenge for healthcare system resilience after an earthquake: The crowdedness of a first-aid hospital by non-urgent patients. *PloS one* 16(4). DOI: 10.1371/journal.pone.0249522.

Lu X, Han B, Hori M, et al. (2014) A coarse-grained parallel approach for seismic damage simulations of urban areas based on refined models and GPU/CPU cooperative computing. *Advances in Engineering Software* 70: 90–103. DOI: 10.1016/j.advengsoft.2014.01.010.

Lu X, Cheng Q, Xu Z, et al. (2019) Real-Time City-Scale Time-History Analysis and Its Application in Resilience-Oriented Earthquake Emergency Responses. *Applied Sciences* 9(17). DOI: 10.3390/app9173497.

Lu X, Cheng Q, Xu Z, et al. (2020) Regional seismic-damage prediction of buildings under mainshock—aftershock sequence. *Frontiers of Engineering Management* (January). DOI: 10.1007/s42524-019-0072-x.

Lupoi A, Cavalieri F and Franchin P (2014) Component Fragilities and System Performance of Health Care Facilities. *Geotechnical, Geological and Earthquake Engineering* 27: 357–384. DOI: 10.1007/978-94-007-7872-6_12.

Marafi NA, Ahmed KA, Lehman DE, et al. (2019) Variability in Seismic Collapse Probabilities of Solid- and Coupled-Wall Buildings. *Journal of Structural Engineering* 145(6). DOI: 10.1061/(ASCE)ST.1943-541X.0002311.

Marafi NA, Makdisi AJ, Berman JW, et al. (2020) Design strategies to achieve target collapse risks for reinforced concrete wall buildings in sedimentary basins. *Earthquake Spectra* 36(3):

1038–1073. DOI: 10.1177/8755293019899965.

Mazzei WJ (1994) Operating room start times and turnover times in a university hospital. *Journal of Clinical Anesthesia* 6(5): 405–408. DOI: 10.1016/S0952-8180(05)80011-X.

Miles SB and Chang SE (2006) Modeling Community Recovery from Earthquakes. *Earthquake Spectra* 22(2): 439–458. DOI: 10.1193/1.2192847.

Mitrani-Reiser J, Mahoney M, Holmes WT, et al. (2012) A Functional Loss Assessment of a Hospital System in the Bío-Bío Province. *Earthquake Spectra* 28(1): 473–502. DOI: 10.1193/1.4000044.

Morley C, Unwin M, Peterson GM, et al. (2018) Emergency department crowding: A systematic review of causes, consequences and solutions. *PloS one* Bellolio F (ed.) 13(8). DOI: 10.1371/journal.pone.0203316.

Morton MJ, DeAugustinis ML, Velasquez CA, et al. (2015) Developments in Surge Research Priorities: A Systematic Review of the Literature Following the Academic Emergency Medicine Consensus Conference, 2007-2015. *Academic Emergency Medicine*. DOI: 10.1111/acem.12815.

Myrtle RC, Masri SF, Nigbor RL, et al. (2005) Classification and prioritization of essential systems in hospitals under extreme events. *Earthquake Spectra* 21(3): 779–802. DOI: 10.1193/1.1988338.

NHERI SimCenter (2018) An Application Framework for Regional Earthquake Simulations. *Natural Hazards Engineering Research Infrastructure (NHERI)*.

NRCC (2015) National Building Code of Canada. *National Research Council Canada (NRCC)*. Available at: https://doi.org/10.4224/40002005.

O'Rourke TD (2007) Critical Infrastructure, Interdependencies, and Resilience. *The Bridge:*

*Linking Engineering and Society* 37(1): 22–29.

Ouyang M (2014) Review on modeling and simulation of interdependent critical infrastructure systems. *Reliability Engineering & System Safety* 121: 43–60. DOI: 10.1016/j.ress.2013.06.040.

Paul JA and Lin L (2012) Models for Improving Patient Throughput and Waiting at Hospital Emergency Departments. *The Journal of Emergency Medicine* 43(6): 1119–1126. DOI: 10.1016/j.jemermed.2012.01.063.

Paul SA, Reddy MC and DeFlitch CJ (2010) A Systematic Review of Simulation Studies Investigating Emergency Department Overcrowding. *Simulation* 86(8–9): 559–571. DOI: 10.1177/0037549710360912.

Pianigiani M, Przelazloski K, Christovasilis IP, et al. (2014) A comprehensive methodology for evaluating the seismic resilience of health care facilities considering nonstructural components and organizational models. In: *Second European Conference on Earthquake and Seismology*, Istanbul, Turkey, 2014.

Poulos A, Favier P, Vásquez J, et al. (2015) Scenario-based seismic performance assessment of a Chilean hospital. In: *Tenth Pacific Conference on Earthquake Engineering Building and Earthquake-Resilient Pacific*, Sydney, Australia, 2015.

Reed DA, Kapur KC and Christie RD (2009) Methodology for Assessing the Resilience of Networked Infrastructure. *IEEE Systems Journal* 3(2): 174–180. DOI: 10.1109/JSYST.2009.2017396.

Schultz CH, Koenig KL and Lewis RJ (2003) Implications of Hospital Evacuation after the Northridge, California, Earthquake. *New England Journal of Medicine* 348(14): 1349–1355. DOI: 10.1056/NEJMsa021807.

Spence R, So E and Scawthorn C (2011) *Human Casualties in Earthquakes*. Advances in Natural and Technological Hazards Research. Dordrecht: Springer Netherlands. DOI: 10.1007/978-90-481-9455-1.

Steelman JS and Hajjar JF (2009) Influence of inelastic seismic response modeling on regional loss estimation. *Engineering Structures* 31(12): 2976–2987. DOI: 10.1016/j.engstruct.2009.07.026.

Taghavi S and Miranda E (2004) Estimation of Seismic Acceleration Demands in Building Components. In: *13th World Conference on Earthquake Engineering Vancouver, B.C., Canada*, Vancouver, B.C., Canada, 2004.

Taghavi S and Miranda E (2005) Approximate Floor Acceleration Demands in Multistory Buildings. II: Applications. *Journal of Structural Engineering* 131(2): 212–220. DOI: 10.1061/(ASCE)0733-9445(2005)131:2(212).

Vásquez A, Rivera F, de la Llera JC, et al. (2017) Healthcare network's response and resilience in Iquique after the 2014, Pisagua earthquake. In: *16th World Conference on Earthquake*, Santiago, Chile, 2017.

Watson SK, Rudge JW and Coker R (2013) Health systems' 'surge capacity': State of the art and priorities for future research. *Milbank Quarterly* 91(1): 78–122. DOI: 10.1111/milq.12003.

Wu C, Chai J-F, Lin C-CJ, et al. (2008) Reconnaissance report of 0512 China Wenchuan earthquake on schools, hospitals and residential buildings. In: *14th World Conference on Earthquake Engineering*, Beijing, China, 2008.

Xiao N, Sharman R, Rao HR, et al. (2012) A simulation-based study for managing hospital emergency department's capacity in extreme events. *International Journal of Business Excellence* 5(1): 140. DOI: 10.1504/IJBEX.2012.044578.

Xiong C, Lu X, Guan H, et al. (2016) A nonlinear computational model for regional seismic simulation of tall buildings. *Bulletin of Earthquake Engineering* 14(4): 1047–1069. DOI: 10.1007/s10518-016-9880-0.

Yavari S, Chang SE and Elwood KJ (2010) Modeling Post-Earthquake Functionality of Regional Health Care Facilities. *Earthquake Spectra* 26(3): 869–892. DOI: 10.1193/1.3460359.

Yi P (2005) Real-time generic hospital capacity estimation under emergency situations. *Thesis Ph.D. State University of New York at Buffalo*. ProQuest Dissertations Publishing.

Yi P, George SK, Paul JA, et al. (2010) Hospital capacity planning for disaster emergency management. *Socio-Economic Planning Sciences* 44(3). Elsevier Ltd: 151–160. DOI: 10.1016/j.seps.2009.11.002.

Yu P, Zhai C and Wen W (2020) A simulation model for estimating hospital capacity during earthquake emergency. In: *17th World Conference on Earthquake Engineering*, Sendai, Japan, 2020.

Zhang X (2018) Application of discrete event simulation in health care: a systematic review. *BMC Health Services Research* 18(1): 687. DOI: 10.1186/s12913-018-3456-4.

Zhong S, Clark M, Hou X, et al. (2014) Development of hospital disaster resilience: conceptual framework and potential measurement. *Emergency Medicine Journal* 31(11): 930–938. DOI: 10.1136/emermed-2012-202282.

Zhu M, McKenna F and Scott MH (2018) OpenSeesPy: Python library for the OpenSees finite element framework. *SoftwareX* 7: 6–11. DOI: 10.1016/j.softx.2017.10.009.

Zsarnoczay A and Kourehpaz P (2020) NHERI-SimCenter/pelicun: v2.6. *Zenodo*. Available at: https://doi.org/10.5281/zenodo.5167371.

# Appendices

## Appendix A

### Validation of NMFS models for RC Shear Wall Buildings

The purpose of this appendix is to demonstrate the step-by-step procedure outline in Section 2.2.3 to build a nonlinear MDOF flexural-shear (NMFS) model of an RC shear wall building, and to validate the reliability and accuracy of the model. A 12-story building subjected to 30 simulated $M_w$.9.0 Cascadia Subduction Zone (CSZ) earthquake ground motions in Seattle, WA is analyzed. Seismic response predictions using the NMFS model are compared with those of a refined finite element (FE) model developed by Marafi *et al.* (2019). The structural performance comparison is presented in terms of periods of vibration, capacity curve, story shears, displacements, story drifts, and floor accelerations. Good agreement is found between the NMFS and the refined FE model.

### A.1 Description of building archetype

The building archetype corresponds to a 12-story RC shear wall building designed to meet the ASCE 7-16 code minimum requirements (Marafi *et al.,* 2019). The typical plan dimension is 30.5m x 30.5m (100ft x 100ft), and a floor-to-floor height of 3.05m (10ft). The lateral resisting system consists of two identical shear walls in the Y direction, as seen in Figure A.1. The concrete was modeled with a specified compressive strength of 55 MPa (~8 ksi) and the rebar with a nominal yield stress of 414 MPa (~60 ksi). The wall length and thickness are constant up the height. The self-weight of the structure and superimposed dead loads is approximated as a uniform load of 6.22 kPa (130 psf) at all levels. Likewise, uniformly distributed live loads are 2.39 kPa (50 psf) at all levels. The calculated seismic weight is 45,542 kN for the typical floor (100% of dead load plus 50% of live load), and the assumed damping ratio is 2.5%. The modulus of elasticity of

concrete, $E_c$ is 30,000 MPa. Also, the cracked section properties of the wall are reduced approximately to 0.5 $I_g$, where $I_g$ is the gross moment of inertia of the cross section. Figure A.1 presents the typical plan view of the shear wall archetype. For the sake of this study, only the cantilevered wall direction will be analyzed.

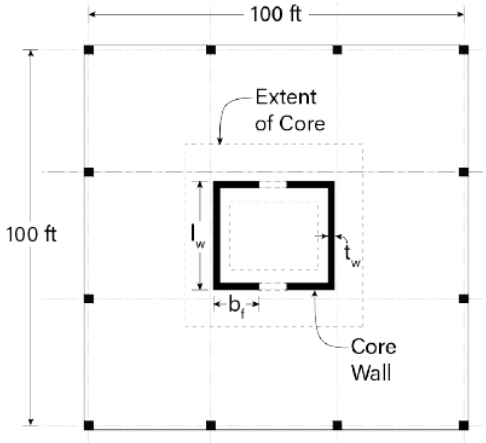


**Figure A.1 Plan view of RC shear wall building at the typical floor (Marafi *et al.*, 2020).**

As shown in Figure A.2, the refined FE model was built using fiber section displacement-based elements and a linear elastic shear spring per story. The material properties include experimentally calibrated values for unconfined and confined concrete. The model was built in OpenSees (McKenna *et al.*, 2010). Further details of the archetype can be found in Marafi *et al.* (2020).

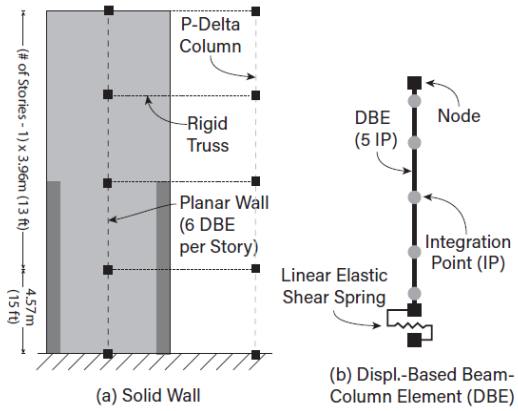


**Figure A.2 Diagram of the OpenSees analytical model illustrating the (a) wall archetype (b) displacement-based elements (Marafi *et al.*, 2020).**

## A.2 Demonstration of the NMFS model calibration procedure

The NMFS model of the 12-story reinforced shear wall building was constructed using OpenSeesPy (Zhu *et al.*, 2018). The parameter calibration follows the procedure described in Section 2.2.3 which is based on Xiong *et al.* (2016):

**Step 1.** Collect the building attribute data:

Based on the previous description of the building archetype, all floors have the same height and mass. The total height, $H$, is $36.56m$ The building type corresponds to a C2H-HC taxonomy (C2: shear wall building type, H: high rise, HC: high code level) according to the HAZUS Technical Manual (FEMA, 2020).

**Step 2.** Calibration of elastic parameters:

The reported periods of the refined FE model were $T_1$=1.808s and $T_2$=0.306s in the shear wall directions. The stiffnesses are assumed to be constant at the building height, and the initial values are estimated as per Taghavi and Miranda (2005). The method relates $T_1$ and $T_2$, by defining a flexural-shear stiffness ratio $\alpha_0$, as shown in Figure A.3. For $T_2/T_1$=0.17, it was found that $\alpha_0 \approx 0.7$. A small value of the ratio ($\alpha_0 < 5$) was found, indicating that deformations are governed by the flexural component as expected of a cantilevered shear wall system.

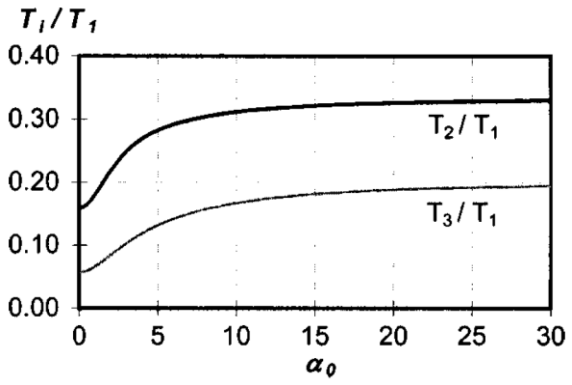


**Figure A.3 Effect of $\alpha_0$ on period ratios of uniform stiffness model (Taghavi and Miranda, 2005).**

Then, by following the procedure outlined by Taghavi and Miranda (2005) that relates $\alpha_0$ to the initial flexural and shear stiffnesses; $EI_0$ and $GA_0$ were obtained:

$$EI_0 = 228{,}179{,}311.5\ kN - m^2 \quad \textit{(A.1)}$$

$$GA_0 = 59{,}154{,}664.5\ kN \quad \textit{(A.2)}$$

After the calibration of the elastic parameters by performing iterative modal analysis of the simplified model to match relevant periods, the flexural stiffness, $EI$, and shear stiffness, $GA$ were calculated. The resulting vibration periods were 1.08s and 0.306s as shown in Table A.1.

$$EI = 264{,}688{,}001.4\ kN - m^2 \quad \textit{(A.3)}$$

$$GA = 47{,}323{,}731.6\ kN \quad \textit{(A.4)}$$

**Table A.1 Vibration periods comparison.**

| Vibration Periods | NMFS model | Refined FE model | Error |
|---|---|---|---|
| $T_1$ | 1.808 s | 1.808 s | 0.0% |
| $T_2$ | 0.306 s | 0.300 s | 2.0% |

**Step 3.** Calibration of yield point:

In this case, since the section dimensions and properties of the wall are available, determining the yield strength by amplifying the design strengths using an overstrength factor (as outlined in Section 2.2.3) was not necessary. Instead, the shear yield strength and yield bending moment were directly calculated from a section analysis performed in Response 2000 software (Bentz and Collins, 2001). Then, the corresponding yield displacement and rotation were calculated using Eq. 2.7 and 2.8, respectively. The calculated yield point parameters at the base ($i = 1$) are:

$$V_{y,1} = 11{,}551.9\ kN \quad \textit{(A.5)}$$

$$M_{y,1} = 64{,}000.0\ kN - m \quad \textit{(A.6)}$$

$$\Delta u_{y,1} = 0.744 * 10^{-3}\, m \quad (A.7)$$

$$\Delta \theta_{y,1} = 0.737 * 10^{-3}\, rad \quad (A.8)$$

**Step 4.** Calibration of peak point:

The peak strengths were derived using the peak overstrength factor, $\Omega_p = 1.8$ given by Table 5.5 of the HAZUS (FEMA, 2020) for a C2H-HC building type. Then, by using Eq. 2.9 and 2.10, we obtained:

$$V_{p,1} = 20{,}793.4\, kN \quad (A.9)$$

$$M_{p,i} = 1152{,}000.0\, kN - m \quad (A.10)$$

Instead of using the stiffness reduction method, the ductility factor method was preferred to determine peak displacements and rotation (Eq. A.11 and A.12). From the pushover curve of the FE model, the ductility was estimated to $\mu = 6.0$.

$$\Delta u_{p,1} = \mu\, \Delta u_{y,1} = 4.464 * 10^{-3}\, m \quad (A.11)$$

$$\Delta \theta_{p,1} = \mu\, \Delta \theta_{y,1} = 4.422 * 10^{-3}\, rad \quad (A.12)$$

**Step 5.** Ultimate strength point:

The ultimate inter-story drift ratio at the Complete Damage state is $\delta_{complete.DS} = 0.04$ as per Table 5.9a of HAZUS (FEMA). Then, the ultimate strength points were calculated using Eq. 2.17 and 2.18:

$$V_{u,1} = V_{p,1} = 20{,}793.4\, kN \quad (A.13)$$

$$M_{u,1} = M_{p,i} = 1152{,}000.0\, kN - m \quad (A.14)$$

$$\Delta u_{u,i} = 0.122\, m \quad (A.15)$$

$$\Delta \theta_{u,1} = 0.04\, rad \quad (A.16)$$

**Step 6.** Hysteretic parameter calibration:

In this study, a uniaxial bilinear hysteretic material object with pinching of force and deformation, and degraded unloading stiffness was used. This material is called "*Hysteretic*" in the OpenSeesPy library. After calibrating the parameters to match the hysteretic behavior of the elements in the FE model, the pinching factors for strain (*pinchX*=0.50), stress (*pinchY*=0.45), and the degraded unloading stiffness (*beta*=0.40) were determined.

The step-by-step procedure presented above corresponds to the parameter calibration at the base level of the building ($i = 1$). To determine the tri-linear backbone curve's control points at the different levels, first, Eq. 2.5 and 2.6 must be used to determine the yield strength of each story. Then, the peak and ultimate strength points for each story are derived by following Steps 3 and 4. Tables A.2 and A.3 summarize the calibrated parameters of the trilinear backbone curve for the nonlinear shear and flexural springs per story.

**Table A.2 Parameters of the trilinear backbone curve for the non-linear shear springs.**

| Story (i) | $V_{y,i}$ (kN) | $\Delta u_{y,i}$ (m) | $V_{p,i}$ (kN) | $\Delta u_{p,i}$ (m) | $V_{u,i}$ (kN) | $\Delta u_{u,i}$ (m) |
|---|---|---|---|---|---|---|
| 1 | 11551.90 | 7.44E-04 | 20793.42 | 4.46E-03 | 20793.42 | 1.22E-01 |
| 2 | 11403.80 | 7.34E-04 | 20526.84 | 4.41E-03 | 20526.84 | 1.22E-01 |
| 3 | 11107.60 | 7.15E-04 | 19993.67 | 4.29E-03 | 19993.67 | 1.22E-01 |
| 4 | 10663.29 | 6.87E-04 | 19193.93 | 4.12E-03 | 19193.93 | 1.22E-01 |
| 5 | 10070.89 | 6.49E-04 | 18127.60 | 3.89E-03 | 18127.60 | 1.22E-01 |
| 6 | 9330.38 | 6.01E-04 | 16794.69 | 3.61E-03 | 16794.69 | 1.22E-01 |
| 7 | 8441.77 | 5.44E-04 | 15195.19 | 3.26E-03 | 15195.19 | 1.22E-01 |
| 8 | 7405.06 | 4.77E-04 | 13329.12 | 2.86E-03 | 13329.12 | 1.22E-01 |
| 9 | 6220.25 | 4.01E-04 | 11196.46 | 2.40E-03 | 11196.46 | 1.22E-01 |
| 10 | 4887.34 | 3.15E-04 | 8797.22 | 1.89E-03 | 8797.22 | 1.22E-01 |
| 11 | 3406.33 | 2.19E-04 | 6131.39 | 1.32E-03 | 6131.39 | 1.22E-01 |
| 12 | 1777.22 | 1.14E-04 | 3198.99 | 6.87E-04 | 3198.99 | 1.22E-01 |

**Table A.3 Parameters of the trilinear backbone curve for the non-linear flexural springs.**

| Story (i) | $M_{y,i}$ (kN-m) | $\Delta\theta_{y,i}$ (rad) | $M_{p,i}$ (kN-m) | $\Delta\theta_{p,i}$ (rad) | $M_{u,i}$ (kN-m) | $\Delta\theta_{u,i}$ (rad) |
|---|---|---|---|---|---|---|
| 1 | 64000.00 | 7.37E-04 | 115200.00 | 4.42E-03 | 115200.00 | 4.00E-02 |
| 2 | 61672.73 | 7.10E-04 | 111010.91 | 4.26E-03 | 111010.91 | 4.00E-02 |
| 3 | 59345.45 | 6.83E-04 | 106821.82 | 4.10E-03 | 106821.82 | 4.00E-02 |
| 4 | 57018.18 | 6.57E-04 | 102632.73 | 3.94E-03 | 102632.73 | 4.00E-02 |
| 5 | 54690.91 | 6.30E-04 | 98443.64 | 3.78E-03 | 98443.64 | 4.00E-02 |
| 6 | 52363.64 | 6.03E-04 | 94254.55 | 3.62E-03 | 94254.55 | 4.00E-02 |
| 7 | 50036.36 | 5.76E-04 | 90065.45 | 3.46E-03 | 90065.45 | 4.00E-02 |
| 8 | 47709.09 | 5.49E-04 | 85876.36 | 3.30E-03 | 85876.36 | 4.00E-02 |
| 9 | 45381.82 | 5.23E-04 | 81687.27 | 3.14E-03 | 81687.27 | 4.00E-02 |
| 10 | 43054.55 | 4.96E-04 | 77498.18 | 2.97E-03 | 77498.18 | 4.00E-02 |
| 11 | 40727.27 | 4.69E-04 | 73309.09 | 2.81E-03 | 73309.09 | 4.00E-02 |
| 12 | 38400.00 | 4.42E-04 | 69120.00 | 2.65E-03 | 69120.00 | 4.00E-02 |

## A.3 Comparison between NMFS model and refined FE model

Table A.1 presented the comparison of the vibration periods and shows a good agreement between the NMFS and the refined FE model. Further, a non-linear static analysis is performed to compare the capacity curves (i.e., Pushover curves) of both models. As seen in Figure A.4 the pushover curve of the NMFS aligns very well with the one of the refined FE model, demonstrating the great accuracy of utilizing tri-linear curves to characterize the non-linear behavior of shear walls.

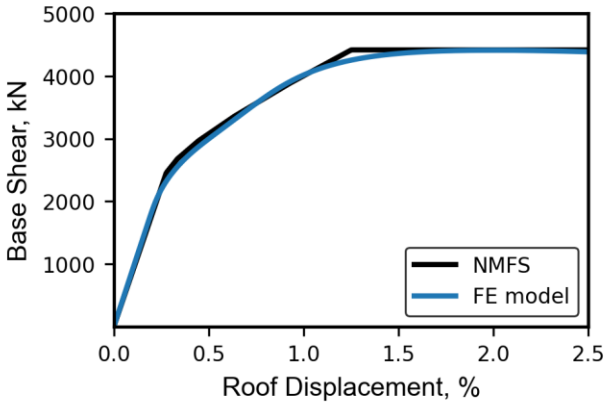


**Figure A.4 Pushover curves comparison of the simplified nonlinear model and the refine FE model of a 12-story RC shear wall building**

To verify the dynamic behavior of the NMFS model, a nonlinear response time history analysis is performed. The ground motions correspond to an $M_w$9.0 CSZ earthquake scenario. A suite of 30 accelerograms was obtained from physics-based ground motion simulations in Seattle, WA performed by Frankel *et al.* (2018). EDPs for the 30 individual simulations and the mean results are presented in Figure A.5. It is observed that the mean story shears and mean floor accelerations align well with the FE model, with variations under 10% throughout the height of the structural model and under 2% for the mean peak values. Meanwhile, the mean story displacements and drift ratios determined using the simplified model vary by under 15% throughout the height of the structural model.

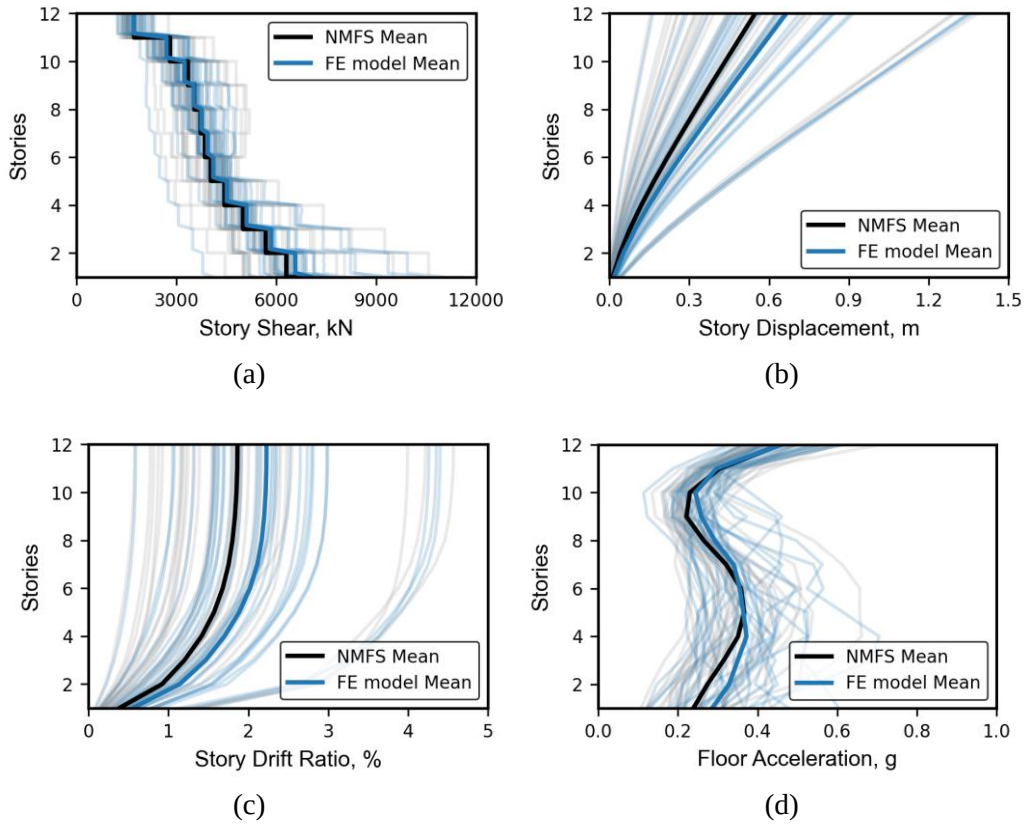


**Figure A.5 Validation of the simplified nonlinear model (a) story shear, (b) story displacement, (c) story drift ratio, and (d) floor acceleration of a 12-story RC shear wall building subjected to 30 $M_w$9.0 CSZ ground motions in Seattle, WA.**

As seen in Figures A.4 and A.5, a good agreement of the structural response (in terms of periods of vibration, pushover curve, story shears, displacements, drifts, and floor accelerations) was found. Further, the simplified model demonstrated its ability to simulate a high level of nonlinearity in the structure, presented specifically in three of the thirty simulations, where the story drift ratio reached values above 4% (See Figure A.5c). The computing efficiency is also remarkably improved, as the simplified NMFS model was 2,500 times faster than the refined FE model when performing the non-linear time history analysis. It is concluded that the NMFS can accurately and efficiently estimate seismic response predictions of RC shear wall systems.

## Appendix B

### Discrete Event Simulation (DES) model for an Emergency Department

The purpose of this appendix is to further illustrate the advantages of using DES modeling and provide complementary details of the Case Study presented in Chapter 4. The post-earthquake capacity of the case study ED is estimated for different probable functionality loss outputs, and an explanation of how to determine the median capacity using the DES model is also provided.

### B.1 DES modeling in JaamSim

In this study, JaamSim (King and Harrison, 2013) was the preferred software to build the DES model because it (1) is an open-source discrete event simulation package, (2) offers a graphical user interface that allows drag-and-drop of pre-defined objects for model building (e.g., entities, queues, probability distributions, etc.) and (3) provides controls for launching and manipulating simulation runs in a very practical way. This last point allowed me, for example, to automatize the run of the 30 simulations (each of those with a different surge in demand and anticipated functionality loss) using a Python script. Likewise, another code was built to perform a sensitivity analysis to determine the capacity during normal and disaster earthquake conditions, as explained in the next section.

The graphical representation of the DES model of the case study hospital ED built-in JaamSim software is shown in Figure B.1. The analyzed ED consists of triage, emergency rooms (ER), laboratories, operating rooms (OR), recovery rooms (RR), and inpatient beds. All these stages are considered in the DES model to estimate patients' wait times and length of stay. The location of the services areas within the hospital building, as defined in Section 4.6, is also shown in the figure. To simulate each service area on the DES model, the following objects had to be defined: entities, servers, queues, resources, time series, branches, probability distributions, and

recorders to measure relevant output data. The path network where entities (i.e., patients) can travel between the defined objects within the ED, follows the patient routing defined in Figure 3.4.

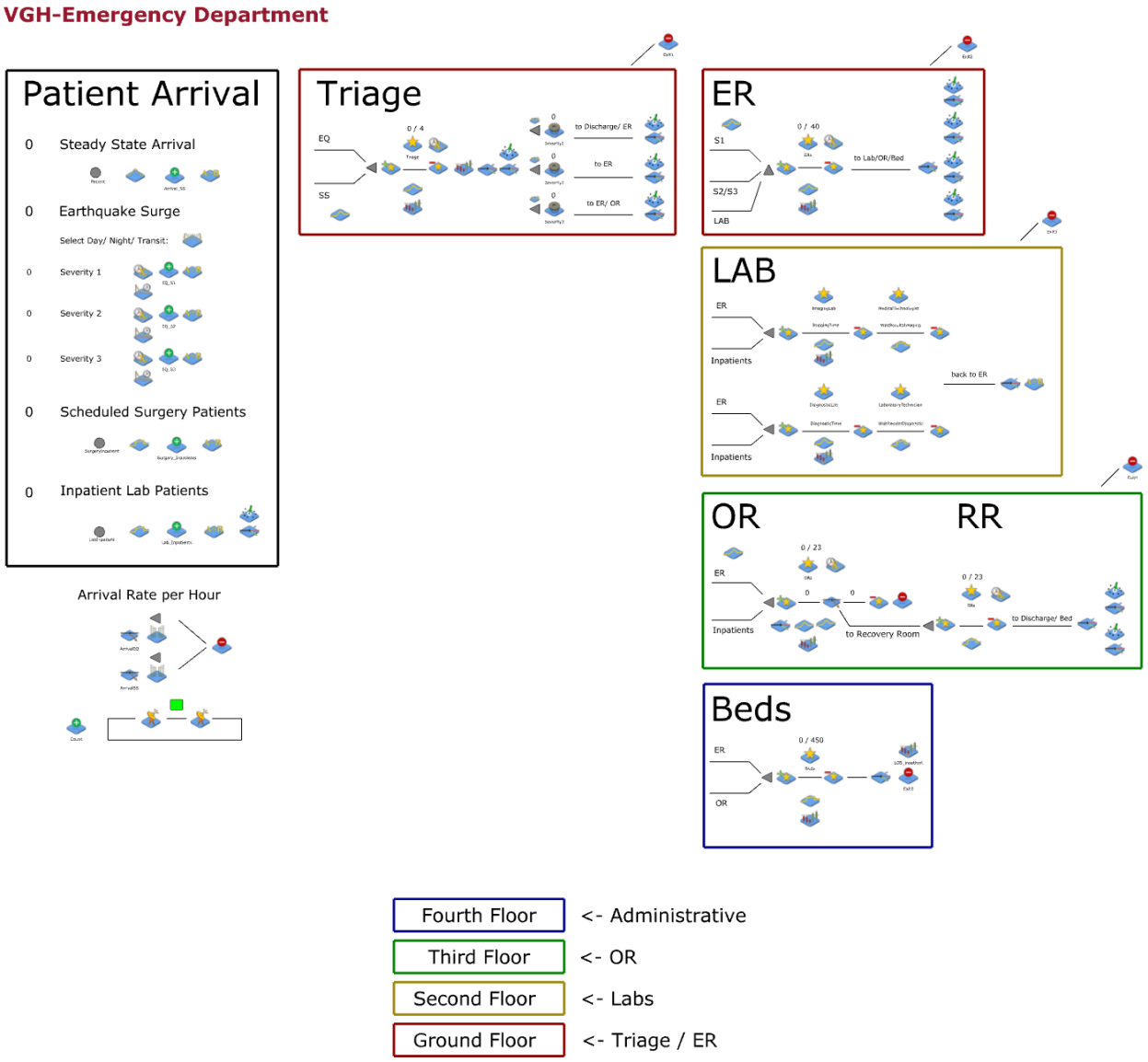


**Figure B.1 Graphical view of the DES model of the VGH emergency department in JaamSim.**

## B.2 Capacity estimation using DES model

Referring back to Section 2.1.2, capacity is defined as the critical arrival rate threshold that an ED cannot exceed. In this study, the hospital capacity is estimated by a sensitivity analysis performed by incrementing the patient arrival rate until the ED is overcrowded (e.g., WTs on triage, laboratories, ERs, ORs exceed the performance threshold of 2 hours). This analysis is performed by leveraging the validated DES model, which is capable of providing ED services' wait times for different patient arrival rates. In the methodology developed, the functionality of a service area is estimated as a function of the damage extents to the structural and non-structural components on the corresponding floor. Then, the overall ED capacity is calculated for the different floor functionality loss combinations, so that the median functionality loss output that characterizes the post-earthquake ED capacity can be determined. This analysis is necessary because, as is demonstrated later in this section, functionality losses of services areas affect the overall ED capacity to varying degrees.

Table B.1 lists the different probable functionality loss outputs for the case study presented in Chapter 4. The location of the treatment areas on each floor of the hospital building can be found in Table 4.3. For each probable output, the capacity in terms of arrival rate (pat./hour) is estimated by sensitivity analysis. The outputs are sorted from the most favorable case (i.e., no functionality loss) to the less favorable cases. As seen in the table, some functionality outcomes lead to the same overall ED capacity. This is because, in the specific case study, the 2$^{nd}$ and 4$^{th}$ floors correspond to laboratories and administrative offices, which do not affect the ED patient flow during the emergency response.

**Table B.1 Probable functionality loss outcomes and corresponding surge capacity.**

| Probable Output No. | 1st floor | 2nd floor | 3rd floor | 4th floor | pat./hour |
|---|---|---|---|---|---|
| 1 | 1.00 | 1.00 | 1.00 | 1.00 | 15.0 |
| 2 | 1.00 | 1.00 | 1.00 | 0.75 | 15.0 |
| 3 | 1.00 | 1.00 | 1.00 | 0.50 | 15.0 |
| 4 | 1.00 | 0.75 | 1.00 | 1.00 | 15.0 |
| 5 | 1.00 | 0.50 | 1.00 | 1.00 | 15.0 |
| 6 | 1.00 | 0.75 | 1.00 | 0.75 | 15.0 |
| 7 | 1.00 | 0.75 | 1.00 | 0.50 | 15.0 |
| 8 | 1.00 | 1.00 | 0.75 | 1.00 | 13.0 |
| 9 | 1.00 | 1.00 | 0.75 | 0.75 | 13.0 |
| 10 | 1.00 | 0.75 | 0.75 | 1.00 | 13.0 |
| 11 | 1.00 | 0.75 | 0.75 | 0.75 | 13.0 |
| 12 | 0.75 | 1.00 | 1.00 | 1.00 | 11.5 |
| 13 | 0.75 | 1.00 | 1.00 | 0.75 | 11.5 |
| 14 | 0.75 | 0.75 | 1.00 | 1.00 | 11.5 |
| 15 | 0.75 | 0.75 | 1.00 | 0.75 | 11.5 |
| 16 | 0.75 | 1.00 | 0.75 | 1.00 | 11.5 |
| 17 | 0.75 | 1.00 | 0.75 | 0.75 | 11.5 |
| 18 | 0.75 | 0.75 | 0.75 | 1.00 | 11.5 |
| 19 | 0.75 | 0.75 | 0.75 | 0.75 | 11.5 |
| 20 | 0.75 | 0.75 | 0.75 | 0.50 | 11.5 |
| 21 | 0.50 | 1.00 | 1.00 | 1.00 | 7.5 |
| 22 | 0.50 | 1.00 | 0.75 | 1.00 | 7.5 |
| 23 | 0.50 | 0.75 | 0.75 | 0.75 | 7.5 |
| 24 | 1.00 | 1.00 | 0.50 | 1.00 | 5.0 |
| 25 | 0.75 | 1.00 | 0.50 | 1.00 | 5.0 |
| 26 | 0.75 | 0.75 | 0.50 | 0.75 | 5.0 |
| 27 | 0.50 | 1.00 | 0.50 | 1.00 | 5.0 |

To illustrate the approach to determine the ‘patient per hour’ overall capacity of the ED, two cases are selected from Table B.1: (1) functionality loss outputs No. 1, which corresponds to the ED during normal conditions (i.e., no functionality loss), and (2) functionality loss outputs No. 8, where a functionality loss of 25% is anticipated on the 3rd floor only. The sensitivity analysis was performed with 0.1 pat./h increments of the patient arrival rate, and a wait time limit for ERs and ORs of 2 hours. Figure B.3 presents the results of the sensitivity analyses to estimate capacity for the functionality loss outputs No. 1. Figure B.2 presents the results of the sensitivity analyses

to estimate capacity for the functionality loss outputs No. 1. It is observed in the figures that, for an iterative increase of the patient arrival rate from 14.9 to 15.3 pat./h, the ER WTs increase dramatically while the other service areas' wait times maintain their steady-state. Thus, ERs were identified to be the bottleneck in the patient flow. From Figure B.2 (a), the overall ED capacity is determined to be 15.0 pat./h, as any increase of this value leads to ER WTs exceeding the limit of 2 hours.

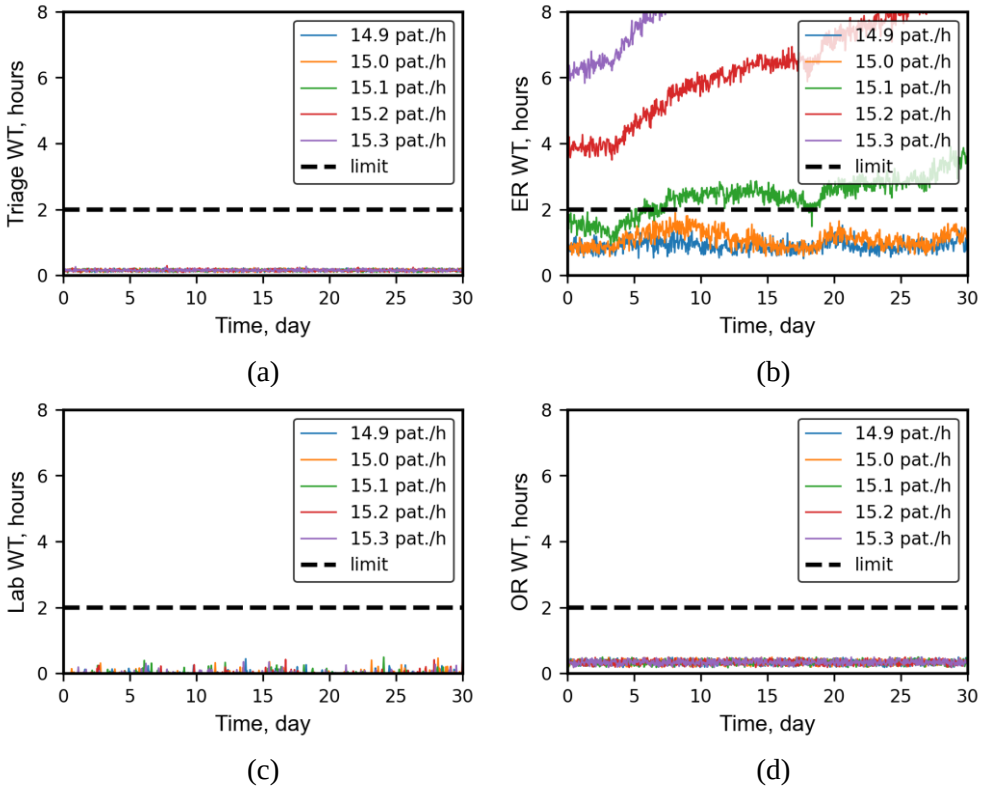


**Figure B.2 Sensitivity analysis to determine ED capacity during normal conditions, including the temporal variation of (a) mean triage wait time, (b) mean emergency room wait time (ER WT), (c) mean laboratory wait times, and (d) mean operating room wait times (OR WT) for incremental arrival rates.**

Likewise, Figure B.3 presents the results of the sensitivity analyses to estimate capacity for the functionality loss outputs No. 8. It is observed in the figures that, for an iterative increase of the patient arrival rate from 12.9 to 13.3 pat./h, the OR WTs increase dramatically while the other

service areas' wait times maintain their steady-state. As expected, ORs were identified to be the bottleneck since are the only service area located on the 3rd floor, where a functionality loss of 25% is anticipated. From Figure B.3 (b), the overall ED capacity is determined to be 13.0 pat./h, as any increase of this value leads to OR WTs exceeding the limit of 2 hours.

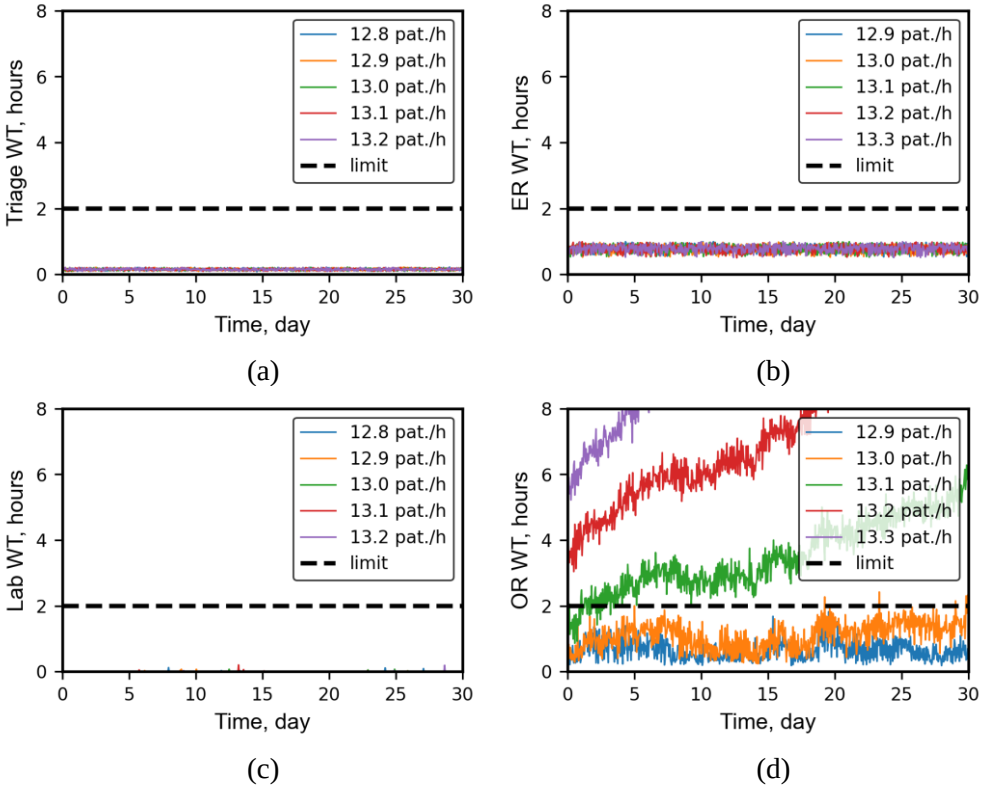


**Figure B.3 Sensitivity analysis to determine ED capacity when ORs are the bottleneck, including the temporal variation of (a) mean triage wait time, (b) mean emergency room wait time (ER WT), (c) mean laboratory wait times, and (d) mean operating room wait times (OR WT) for incremental arrival rates.**

Given the earthquake intensity level at the location of the case study ED (refer to Figure 4.1), the probable functionality loss outputs listed in Table B.1 were sufficient to find the median (50th percentile) capacity of the 30 $M_w$9.0 CSZ earthquake scenarios considered. If a more unfavorable scenario were anticipated in terms of expected damage and consequent functionality loss (e.g., due

to poor seismic performance of the hospital building), Table B.1. might need to be extended to consider more unfavorable outputs in order to find the median capacity.

**Table B.2 Median capacity and functionality per floor for the 30 $M_w$9.0 CSZ ground motion scenarios.**

| Scenario | 1st Story | 2nd Story | 3rd Story | 4th Story | Pat./hour |
|---|---|---|---|---|---|
| 1 | 1.00 | 0.75 | 0.75 | 0.75 | 13.0 |
| 2 | 1.00 | 1.00 | 0.75 | 1.00 | 13.0 |
| 3 | 1.00 | 0.75 | 0.75 | 0.75 | 13.0 |
| 4 | 1.00 | 1.00 | 1.00 | 0.75 | 15.0 |
| 5 | 1.00 | 1.00 | 0.75 | 1.00 | 13.0 |
| 6 | 1.00 | 1.00 | 0.75 | 1.00 | 13.0 |
| 7 | 1.00 | 1.00 | 1.00 | 0.75 | 15.0 |
| 8 | 1.00 | 1.00 | 1.00 | 0.75 | 15.0 |
| 9 | 1.00 | 1.00 | 1.00 | 1.00 | 15.0 |
| 10 | 0.75 | 1.00 | 1.00 | 0.75 | 11.5 |
| 11 | 1.00 | 1.00 | 1.00 | 0.75 | 15.0 |
| 12 | 1.00 | 0.75 | 1.00 | 0.75 | 15.0 |
| 13 | 1.00 | 1.00 | 0.75 | 1.00 | 13.0 |
| 14 | 1.00 | 1.00 | 0.75 | 1.00 | 13.0 |
| 15 | 1.00 | 1.00 | 1.00 | 1.00 | 15.0 |
| 16 | 1.00 | 1.00 | 0.75 | 1.00 | 13.0 |
| 17 | 0.75 | 0.75 | 0.75 | 0.75 | 11.5 |
| 18 | 1.00 | 0.75 | 1.00 | 0.75 | 15.0 |
| 19 | 1.00 | 1.00 | 0.75 | 0.75 | 13.0 |
| 20 | 1.00 | 1.00 | 1.00 | 0.75 | 15.0 |
| 21 | 0.75 | 0.75 | 0.75 | 0.75 | 11.5 |
| 22 | 0.75 | 0.75 | 0.75 | 0.75 | 11.5 |
| 23 | 1.00 | 1.00 | 1.00 | 0.75 | 15.0 |
| 24 | 0.75 | 0.75 | 0.75 | 0.75 | 11.5 |
| 25 | 1.00 | 1.00 | 1.00 | 0.75 | 15.0 |
| 26 | 1.00 | 1.00 | 0.75 | 0.75 | 13.0 |
| 27 | 1.00 | 1.00 | 0.75 | 0.75 | 13.0 |
| 28 | 0.75 | 0.75 | 0.75 | 0.75 | 11.5 |
| 29 | 1.00 | 1.00 | 0.75 | 1.00 | 13.0 |
| 30 | 0.75 | 0.75 | 0.75 | 0.75 | 11.5 |

For the case study, Table B.2 presents the median capacity and the corresponding functionality loss per floor for the 30 $M_w$9.0 ground motion scenarios. The median capacity results, listed in the last column of the table, were also presented in a bar chart format in Figure 4.5. From Table B.2, it is observed that in 11 out of the 30 scenarios, the median capacity equals the capacity of the model 15.0 pat./hour during normal conditions, indicating that no functionality loss is

observed in those scenarios. On the other hand, the most unfavorable case is observed in 7 out of the 30 scenarios, where the capacity equals 11.5 pat./hour. It is important to point out that these functionality loss results are not dependent on the earthquake occurrence time during the day.